Science of the Total Environment 864 (2023) 160901

Contents lists available at ScienceDirect

Science of the Total Environment

journal homepage: www.elsevier.com/locate/scitotenv

# Plastic leachate-induced toxicity during sea urchin embryonic development: Insights into the molecular pathways affected by PVC

Periklis Paganos [a], Clemens Vinzenz Ullmann [b], Daniela Gaglio [c,e], Marcella Bonanomi [d,e], Noemi Salmistraro [c,e], Maria Ina Arnone [a,*], Eva Jimenez-Guri [a,f,*]

[a] Stazione Zoologica Anton Dohrn, Department of Biology and Evolution of Marine Organisms, Naples, Italy
[b] Department for Earth and Environmental Sciences, Faculty of Environment, Science and Economy, University of Exeter, Penryn Campus, Penryn, UK
[c] Institute of Molecular Bioimaging and Physiology (IBFM), National Research Council (CNR), Segrate, Milan, Italy
[d] Department of Biotechnology and Biosciences, University of Milano-Bicocca, Milan, Italy
[e] ISBE, IT/Centre of Systems Biology-Elixir Infrastructure and NBFC, National Biodiversity Future Center, Palermo, Italy
[f] Centre for Ecology and Conservation, University of Exeter, Cornwall Campus, Penryn, UK

## HIGHLIGHTS

- Sea urchin development is disturbed by plastic particle leachates.
- Abnormalities include radialisation; skeleton, neural and immune cells malformation.
- Transcriptomics reveal altered gene expression determining malformed structures.
- Metabolomics show high redox stress; low mitochondria activity and DNA/RNA synthesis.
- PVC leachates have high concentrations of zinc.

## GRAPHICAL ABSTRACT

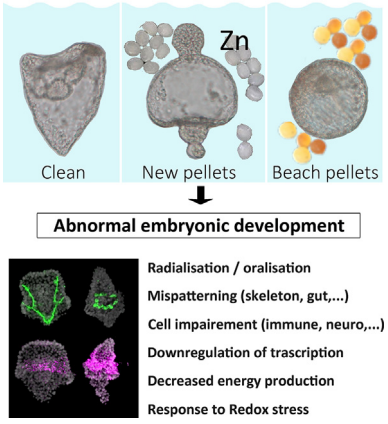


## ARTICLE INFO

Editor: Kevin V Thomas

*Keywords:*
Microplastic
Leachates
Ecotoxicology
Embryonic development
Sea urchin
Gene regulation
Zinc

## ABSTRACT

Microplastics are now polluting all seas and, while studies have found numerous negative interactions between plastic pollution and marine animals, the effects on embryonic development are poorly understood. A potentially important source of developmental ecotoxicity comes from chemicals leached from plastic particles to the marine environment. Here we investigate the effects of leachates from new and beach-collected pellets on the embryonic and larval development of the sea urchin *Strongylocentrotus purpuratus* and demonstrate that exposure of developing embryos to these leachates elicits severe, consistent and treatment-specific developmental abnormalities including radialisation of the embryo and malformation of the skeleton, neural and immune cells. Using a multi-omics approach we define the developmental pathways disturbed upon exposure to PVC leachates and provide a mechanistic view that pinpoints cellular redox stress and energy production as drivers of phenotypic abnormalities following exposure to PVC leachates. Analysis of leachates identified high concentrations of zinc that are the likely cause of these observed defects. Our findings point to clear and specific detrimental effects of marine plastic pollution on the development of echinoderms, demonstrating that chemicals leached from plastic particles into sea water can produce strong developmental abnormalities via specific pathways, and therefore have the potential to impact on a wide range of organisms.

* Corresponding authors at: Stazione Zoologica Anton Dohrn, Department of Biology and Evolution of Marine Organisms, Naples, Italy
*E-mail addresses:* periklis.paganos@szn.it (P. Paganos), c.ullmann@exeter.ac.uk (C.V. Ullmann), daniela.gaglio@ibfm.cnr.it (D. Gaglio), marcella.bonanomi@unimib.it (M. Bonanomi), noemi.salmistraro@ibfm.cnr.it (N. Salmistraro), miarnone@szn.it (M.I. Arnone), eva.jimenez-guri@szn.it (E. Jimenez-Guri).

http://dx.doi.org/10.1016/j.scitotenv.2022.160901
Received 5 August 2022; Received in revised form 8 December 2022; Accepted 8 December 2022
Available online 13 December 2022

## 1. Introduction

Plastic pieces are an ever-growing pollutant and have been most extensively studied in the marine environment (Eriksen et al., 2014; Thushari and Senevirathna, 2020), threatening marine ecosystems by several mechanisms, at different life stages and affecting a large swathe of animals (Wright et al., 2013). Microplastics (plastic particles smaller than 5 mm) can come from the degradation of bigger plastic items lost in the environment, such as plastic bottles or bags. They can also be purposely made small, or derived from abrasion during manufacturing or use (Sundt and Per-Erik Schultze, 2014), arriving to the environment already as small plastic particles. Examples of the latter, known as primary microplastics, are plastic preproduction pellets, cosmetic microbeads and abrasion particles from synthetic textiles and tyres (Boucher and Friot, 2017; Rochman et al., 2019).

Plastic pre-production pellets are the raw material used in the manufacture of plastic items. Shaped similarly to lentils, these small, typically 2–5 mm in diameter (Karlsson et al., 2018), plastic beads are made from any type of plastic polymer and shipped around the world to their destination factories to produce everything from water bottles to drain pipes and garden furniture. In the producing process, these plastic nurdles are supplemented with different types of chemical additives that will act as plasticisers (such as phthalate esters), stabilisers or antioxidants, among others. Unfortunately, accidental loss of these pellets during manufacture, processing and transport is not uncommon (Essel et al., 2015; Karlsson et al., 2018), with first occurrences being reported 50 years ago (Carpenter and Smith, 1972; Carpenter et al., 1972).

Around 230,000 t of nurdles end up in the ocean every year (Sherrington, 2016), and in the UK only, between 5 and 53 billion pellets are estimated to be lost from production plants (Cole and Sherrington, 2016). Some recent spills have had catastrophic consequences for the environment around the spill site, and after, these beads can be found hundreds of miles away and in other territories (van der Molen et al., 2021). A recent example of such an environmental tragedy is the Express pearl disaster in Sri Lanka in 2021 (Sewwandi et al., 2022), but a few more are worth noting (recently, South Africa 2020 and 2018, North Sea 2019 and 2020). Once in the water, fish and other animals can ingest these particles by mistake, and they can end up in their digestive tracts (Carpenter et al., 1972; Provencher et al., 2015). Moreover, not only can they leach the native additives, but they are also capable of adsorbing persistent organic pollutants, transporting them, and later releasing them back into the water (Teuten et al., 2009; Engler, 2012; Gauquie et al., 2015; Rendell-Bhatti et al., 2020). At the spill site, the concentration of plastic can be overwhelming, and due to the potential high concentration of toxic leachates it is very important to understand the short-term effect of these leachate additives for marine life. It is also of interest to know the evolution of the hazardous nature of the particle if it stays in the water and has a longer life at sea. One particularly sensitive life stage is during early development when, rather than being affected by consumed plastics, the toxic effects occur through the leaching of chemicals into the water (Li et al., 2016; Oliviero et al., 2019; Rendell-Bhatti et al., 2020; Gardon et al., 2020).

Development is highly regulated, and the processes involved are highly conserved in the animal kingdom. Fertilisation of gametes and development of marine embryos mostly occur in the water, and in the case of invertebrates, this is usually a very fast process. Hence, exposure to high concentrations of plastic leachates, which are not expected in normal marine environments, during early life stages may lead to impairment of normal embryo development and populations might decrease as a consequence of reduced recruitment.

Sea urchins are ideal experimental systems to investigate such consequences, due to the stereotypic development of their embryos and early larvae, the availability of genetic resources and the detailed description of their cell type repertoire (Angerer and Davidson, 1984; Andrew Cameron and Davidson, 1991; Ernst, 2011; Massri et al., 2021; Paganos et al., 2021). Importantly, sea urchin embryos offer the possibility to untangle the molecular mechanisms related to a given phenotype as a result of gene perturbation or exposure to different substances, due to the fact that most gene regulatory networks (GRNs) controlling axial establishment, as well as the specification and differentiation of most of its cell types, have been reconstructed in great detail (Li et al., 2012; Annunziata and Arnone, 2014; Andrikou et al., 2015; Arnone et al., 2016; Martik et al., 2016; Ettensohn, 2020).

We have previously shown strong developmental abnormalities caused by plastic leachates in the sea urchin *Paracentrotus lividus* (Rendell-Bhatti et al., 2020). One of the most severe phenotypes was caused by PVC leachates that induced deficits in neurogenesis, skeletogenesis and axial patterning, but the mechanistic processes behind those have not been studied. Here, we use a multi-omics approach to unravel the molecular mechanisms and pathways affected by the exposure of embryos and larvae of the sea urchin *Strongylocentrotus purpuratus* to PVC leachates. In detail, we performed differential RNA sequencing (deRNA-seq) on embryos/larvae reared in normal filtered seawater (FSW) and in PVC leached FSW. Next, by taking advantage of the already established *S. purpuratus* larvae cell type family atlas (Paganos et al., 2021) we mapped the differentially transcribed genes into distinct domains of the embryo and larva to uncover which are the specific cell types and GRNs affected. In parallel, we performed metabolomic profiling of the PVC leachate-treated specimens and in combination with deRNA-seq we reconstructed the precise metabolic pathways affected in response to the leachates. Finally, chemical analysis of the PVC leachates revealed the presence of contaminants in the water, all in all providing evidence of the impact of PVC contamination on marine life.

## 2. Materials and methods

### 2.1. Animal husbandry and fertilisation

Adult *S. purpuratus* were housed in circulating seawater at 14 °C, to prevent them from spontaneous spawning, in the aquarium facility of the Stazione Zoologica Anton Dohrn, Naples (Italy). Gamete release was induced by vigorously shaking ripe animals. Eggs were cleaned of any debris by filtering through 100 μm mesh. For each fertilisation, 5 μl of dry sperm was diluted with 13 ml of Filtered Seawater (FSW) and eggs were fertilised by adding 5 drops of the diluted sperm in single crossings. Fertilisation success was checked to ensure the elevation of the fertilisation membrane in >95 % of eggs. Embryos and larvae were let to develop at 15 °C in 9:1 diluted FSW (9 parts filtered Mediterranean Sea seawater, 1 part distilled water) to reach the appropriate salinity of approximately 35 ppt.

### 2.2. Generation of microplastic leachates and embryo exposure

Plastic particles were used to obtain leachates. Beach pellets were collected from Cornwall, UK. These pellets were separated in two classes: Nurdles and Biobeads, and were manually sorted from other plastics and organic matter. Nurdles are the pre-production plastic material that feeds any factory making plastic products, and can be of any type of plastic available (Mato et al., 2001). Biobeads are floating filters of the same size as nurdles but with a rugged edge to increase surface area to aid their filtering properties. They are made of plastics recycled from end-of-life electrical and electronic material and are used in water treatment plants in the South west of England, among other places (Turner et al., 2019). Commercial PVC nurdles (from now on just referred to as PVC) purchased from Northern Polymers and Plastics Ltd. (UK) were used as non-environmental pellets. We obtained the microplastic leachates from these plastic pellets as described in (Rendell-Bhatti et al., 2020) with slight modifications. In brief, plastic pellets were added to filtered seawater (0.22 μm) at a concentration of 10 % (*v*/v). Pellets were leached for 72 h on a Heidolph orbital platform shaker (Heidolph Unimax 2010), with continuous shaking at room temperature (ca 18 °C) in the dark. Leachates were obtained by filtering through filter paper in order to remove particles. Leachates were diluted to the final concentration in filtered seawater (0.22 μm).

Embryos were added to treatment beakers, containing 500 ml of microplastic leachate or control FSW, at a density of 50 embryos per ml, immediately after confirmation of fertilisation success and left to develop in a static incubator at 15 °C on a 12:12 light dark cycle until the desired stage (48 or 72 hpf). Plastic particle concentrations in the treated water ranged between 1 % and 10 %.

### 2.3. Transcriptome sequencing and expression analysis

Three batches of control and 10 % PVC leachate-treated embryos were used to obtain RNA samples at 48 hpf and 72 hpf. Each sample was composed of thousands of embryos/larvae. All samples were snap frozen in liquid nitrogen and stored at −80 °C. Total RNA was extracted using the Qiagen Rneasy Mini kit with Dneasy column following the manufacturer's specifications. RNA concentration and quality were assessed using a nanodrop (Invitrogen) and integrity was visualised in an agarose gel. These six RNA samples were processed at Genomix 4 Life (Salerno, Italy). After quality assessment, TruSeq standard mRNA libraries were prepared and sequencing was performed with an Illumina NextSeq 500 platform using 75 bp paired-end sequencing. The samples were mapped onto the newest reference genome (Spur v5.0) obtained from Echinobase (Arshinoff et al., 2022) using STAR (version 2.7.5c) (Dobin et al., 2013), with the standard parameters for paired reads. The transcriptomic sequences have been deposited at GenBank under BioProject ID PRJNA890282. The quantification of transcripts expressed for each sequenced sample was performed using FeatureCounts algorithm (version 2.0) (Liao et al., 2014). R was used to create a matrix of all genes expressed in all samples with the corresponding read-counts and the data were normalised in a Bioconductor package DESeq2 (Love et al., 2014), using the median of ratio to perform the differential expression analysis between control and treated samples at each time point. To evaluate the general similarity between the samples, we performed Principal Component Analysis (PCA) among all samples in each condition considered using pheatmap and ggplot2, integrated into the package DESeq2. An output table of differential expression for each comparison was made with DESeq2 (Love et al., 2014). Gene expression changes were further visualised using the pheatmap and ggplot2 R packages. Gene ontology (GO) enrichment analysis was carried out using ShinyGO 0.76 (Ge et al., 2020) to identify overrepresented GO terms from up-and down-regulated genes of PVC treated embryos at both time points. Significant GO terms were identified using the Revigo tool, which also allowed to reduce terms by removing redundant terms and to visualise the data organised by semantic similarity (Supek et al., 2011).

### 2.4. Fluorescent in situ hybridisation (FISH)

Embryos and larvae were fixed and stained as described in Paganos et al., 2022. Briefly embryos and larvae were fixed in 4 % PFA in MOPS Buffer overnight (ON) at 4 °C. Specimens were washed with MOPS Buffer several times and stored in 70 % EtOH in −20 °C. Antisense probes were transcribed from linearized DNA as described in (Perillo et al., 2021) and labelled using Digoxigenin (Roche) or Fluorescein (Roche) following the manufacturer's instructions. We used the following genes specific to particular cell types: *Sp-Pks1* (Perillo et al., 2020), *Sp-Chordin*, *Sp-Nodal*, *Sp-Spec1A*, *Sp-Fbsl_2*, *Sp-FoxABL*, *Sp-Bra*, *Sp-Otp*, *Sp-Tph*, *Sp-Hbn*, *Sp-Fgf9/16/20*, *Sp-Pdx1*, *Sp-Cdx*, *Sp-Rhox3* and *Sp-SoxC* (Paganos et al., 2021), Sp-Ets1 (Rizzo et al., 2006), *Sp-Syt1* (Burke et al., 2006), *Sp-ManrC1A* (Annunziata and Arnone, 2014), *Sp-Ptf1a* and *Sp-Cpa2L* (Perillo et al., 2016). Specimens were hybridised with the respective probes ON at 65 °C. Anti-Digoxigenin or Anti-Fluorescein antibodies, depending on which substrate was used to label the probe, were used at a dilution 1:1000 in PerkinElmer blocking reagent and incubated for 1 h at 37 °C. Signal was amplified using the TSA amplification system (Akoya Biosciences, Cat. #NEL752001KT). Embryos and larvae were mounted with DAPI for imaging with a Zeiss 700 confocal microscope. Images were analysed using FiJi.

### 2.5. Immunohistochemistry (IHC)

Immunohistochemical detections of Msp130 (gift from Dr. McClay) labelling skeletogenic cells (Harkey et al., 1992), Myosin Heavy Chain (MHC-PRIMM, Italy) labelling the esophageal muscles (Andrikou et al., 2015) and β-tubulin marking cilia and cell membranes (Thompson et al., 2021) were performed as described in (Perillo et al., 2021). Dilution factor for anti-Msp130 was 1:20, for anti-MHC (1:50) and for anti-β-tubulin (1:200) in MOPS Buffer containing 1 mg/ml Bovine Serum Albumin (BSA) and 4 % sheep serum (SS). Specimens were washed several times in MOPS buffer and incubated for 1 h at room temperature (RT) with the appropriate secondary antibody (AlexaFluor) diluted 1:1000 in MOPS Buffer. Next, embryos and larvae were washed several times with MOPs buffer and mounted with DAPI for imaging with a Zeiss 700 confocal microscope.

### 2.6. Identification of the cell types affected through scRNA-seq

The cell type family enrichment of the differentially expressed genes of PVC leachate treated embryos and larvae was estimated using available scRNA-seq data. The average score of the differentially expressed genes was estimated at 48 hpf gastrula (unpublished data, Arnone lab) and 72 hpf early pluteus larva (Paganos et al., 2021) and represented as dotplots, generated in R (version 4.1.1) using the DotPlot function incorporated into the Seurat R package (version 4.0.2) (Hao et al., 2021). Each dotplot shows the average score of the differentially expressed genes (log2FC ≥ 1.5) in distinct cell type families as well as the percentage of expressing cells.

### 2.7. Metabolites extraction

Embryos were collected at the same time and as described in Section 2.3. Pellets were washed with NaCl 0.9 % and quenched with 500 μl ice-cold 70:30 acetonitrile:water. Samples were placed at −80 °C for 10 min, then sonicated 5 s for 5 pulses at 70 % power for four times. Samples were centrifuged at 12,000*g* for 10 min and supernatants were collected in a glass insert and dried in a centrifugal vacuum concentrator (Concentrator plus/Vacufuge plus, Eppendorf) at 30 °C for about 2.5 h. Samples were then resuspended with 150 μl $H_2O$ prior to analyses.

### 2.8. LC-MS metabolic profiling

LC separation was performed using an Agilent 1290 Infinity UHPLC system and an InfintyLab Poroshell 120 PFP column (2.1 × 100 mm, 2.7 μm; Agilent Technologies). Mobile phase A was water with 0.1 % formic acid. Mobile phase B was acetonitrile with 0.1 % formic acid. The injection volume was 10 μl and LC gradient conditions were: 0 min: 100 % A; 2 min: 100 % A; 4 min: 99 % A; 10 min: 98 % A; 11 min: 70 % A; 15 min: 70 % A; 16 min: 100 % A with 5 min of post-run. Flow rate was 0.2 ml/min and column temperature was 35 °C. MS detection was performed using an Agilent 6550 iFunnel Q-TOF mass spectrometer with Dual JetStream source operating in negative ionisation mode. MS parameters were: gas temp: 285 °C; gas flow: 14 l/min; nebulizer pressure: 45 psig; sheath gas temp: 330 °C; sheath gas flow: 12 l/min; VCap: 3700 V; Fragmentor: 175 V; Skimmer: 65 V; Octopole RF: 750 V. Active reference mass correction was done through a second nebulizer using masses with *m/z*: 112.9855 and 1033.9881, dissolved in the mobile phase 2-propanol–acetonitrile–water (70:20:10 *v*/v). Data were acquired from m/z 60–1050. Data analysis and isotopic natural abundance correction were performed with MassHunter ProFinder (Agilent Technologies). Relative metabolites abundance was carried out after normalisation using Reserpin internal standard and protein content and statistical analyses were performed using Mass Profiler Professional (Agilent Technologies) (Bonanomi et al., 2021). Raw data is provided in Supplementary file 2. The circos plot was generated with CIRCOS (Krzywinski et al., 2009) to

show the identified down-regulated genes and pathways belonging to the same KEGG pathways.

### 2.9. Microplastic leachate chemical analysis by inductively coupled plasma – optical emission spectrometry (ICP-OES)

Leachates were obtained as explained above. Leachates of 10 % biobeads, nurdles and PVC plastics were gravimetrically diluted c. 1:200 using 50 ml centrifuge tubes in 2 % Nitric Acid in order to adjust the sample matrix for optimal analytical conditions.

Analyses were carried out using an Agilent 5110 VDV Inductively Coupled Plasma Optical Emission Spectrometer (ICP-OES). From initial qualitative measurements of metals that could be detrimental to larval development (Cd, Co, Cr, Cu, Mn, Pb, Sn, V and Zn), only Zn was found in significant concentration and subsequently quantified. Zn concentrations were quantified using a set of three synthetic calibration solutions prepared from a single element certified Zn plasma standard covering a concentration range of 10.8 to 53.3 ng/g and a blank, all of which were doped for matrix matching with 0.5 wt% of natural seawater. The seawater was collected in the Carrick Roads near Mylor Yacht Harbour (50°11′0″N; 5°02′32″W) on June 21st 2022. Matching sensitivity and absence of Zn in natural seawater were confirmed by an equivalent second calibration set made from the same single element plasma standard that was not doped with seawater. The Zn signal was quantified using the 213.857 nm line, yielding an effective detection limit (3 s.d. of baseline readings) of c. 0.06 μg/g in solution when accounting for the 1:200 dilution of the samples. In the absence of a certified standard for Zn in seawater, two synthetic solutions with 26.65 ng/g (1st batch run) and 25.67 ng/g (2nd batch run) Zn that were gravimetrically prepared from a certified Zn plasma standard doped with 0.5 wt% seawater from Carrick Roads was used to ascertain consistency of the results. The first quality control solution reproduced to 26.54 ± 0.19 ng/g (2 s.d., $n = 9$) and the second to 26.79 ± 0.15 ng/g (2 s.d., $n = 8$) ng/g, indicating analytical bias <1 % and repeatability within 1 % (2 r.s.d.) for concentrations much greater than detection limit. As unknowns had lower Zn concentrations of <6 ng/g Zn (<1.2 μg/g equivalent), uncertainty of individual Zn measurements in unknowns is better reflected by the stability of signal intensity which was determined in 12 blocks of 5 s, yielding typical standard errors of the mean (2 s.e.) equating to 13 ng/g. In addition to quantitative Zn measurements, intensities of Ca (317.933 nm, 422.673 nm), Mg (279.553 nm, 280.270 nm, 285.213 nm), Na (589.592 nm), Sr (407.771 nm, 421.552 nm), S (181.972 nm) and Ba (455.403 nm) were monitored to verify the consistency of the sample dilution, and to test for possible presence of Ba.

Variability of experimental results and in natural seawater was further controlled by analysing 4 independent leachate replicates of each treatment and seawater samples.

## 3. Results and discussion

### 3.1. Phenotypic assessment of the S. purpuratus embryos and larvae upon rearing in plastic leachates

We exposed *S. purpuratus* fertilised eggs to leachates from new and beach-collected pellets and assessed the phenotypes observed at 48 and 72 hpf as described in the Materials and methods section. At the gastrula stage, we could already observe deficient development. At 72 hpf, none of the treated embryos had developed into a proper pluteus larva (Fig. 1), with typical characteristics such as pyramidal body shape, tripartite gut, skeletal rods and well-formed ciliary band (Fig. 1. A). Instead, we observed totally radialised larvae in all plastic treatments, with a clear exogastrula phenotype with an apical outgrowth in the 10 % PVC treatment (Fig. 1. B), and spherical larvae with no other distinguishable phenotypic characteristics than a rudimentary internal gut in the 10 % nurdle and biobead treatments (Fig. 1. C, D). Lower nurdle and biobead concentration treatments did not show aberrant phenotypes, but abnormal phenotypes were still obtained as we decreased the concentration of PVC. The phenotype changed to an internal through gut with an apical outgrowth at 5 % (Supplementary Fig. S1. C), and a through gut and no outgrowth at 1 % (Supplementary Fig. S1. B). These consistent concentration specific phenotypes were far from the wild type pluteus larvae found in the controls (Supplementary Fig. S1. A).

These results are consistent with those observed previously in *P. lividus*, where beached and PVC pellet leachates elicited changes including abnormal gastrulation, impaired skeletogenesis, abnormal neurogenesis and embryo radialisation (Rendell-Bhatti et al., 2020), indicating that these types of developmental abnormalities may not be species-specific but affect the whole clade similarly. The PVC treatment-induced phenotype was of particular interest as it clearly resembles the one obtained when the specification of the secondary axis of the sea urchin embryo (oral-aboral) is disturbed. Similar to our *P. lividus* data (Rendell-Bhatti et al., 2020), embryos exposed to PVC leachates are unable to produce a proper skeleton. In normal gastrula embryos, skeletogenic cells are spatially organised around the archenteron, forming a syncytium to which biominerals are deposited (Fig. 2. E). At the pluteus stage, the larval skeleton consists of different skeletal rods that are responsible for the characteristic shape of the larvae (Fig. 2. F). PVC leachate-treated *S. purpuratus* gastrulae seem to be missing differentiated skeletogenic cells as indicated by the absence of the skeletal marker MSP130 immunoreactivity (Fig. 2. I), while the same marker at 72 hpf reveals the presence of radialised syncytium of differentiated skeletogenic cells (Fig. 2. J). Another visible abnormality of the treated larvae is the absence of a well-formed ciliary band, an observation confirmed by the β-tubulin staining showing a reduced ciliary surface when compared to controls (Fig. 2. G, H). Esophageal muscles originate from myoblasts that at gastrula stage populate the tip of the embryonic foregut and at the pluteus stage they differentiate towards circumesophageal muscles controlling the contraction of the sea urchin esophageal region and therefore feeding (Andrikou et al., 2013, 2015). Immunohistochemical staining for the esophageal muscles marker Sp-MHC revealed that exogastrulated larvae are lacking any muscular structure suggesting that exogastrulation impaired muscle development (Fig. 2. K, L).

In the Rendell-Bhatti et al. (2020) study we found PCB and PAH in the leachates of environmental samples, and PAH and HCB in PVC leachates, which we suggested were the possible causes of the malformations observed (Rendell-Bhatti et al., 2020). We had not observed exogastrulas before, but another study had found otherwise well-formed *P. lividus* pluteus larvae with everted gut rudiments when exposed to micronized plastic toys (Oliviero et al., 2019). However, the phenotypes here observed in the PVC treatments clearly mirror phenotypes from classical and new experiments exposing *S. purpuratus* and other sea urchins to heavy metals (Mitsunaga and Yasumasu, 1984; Kobayashi and Okamura, 2004; Cunningham et al., 2020), as well as to oral-aboral axis formation disorganisation (Duboc et al., 2004). Indeed, we see radialised/oralised embryos similar to those described when the developmental pathways involved in oral/aboral (O/A) and left/right (L/R) axis formation are disrupted (Duboc et al., 2004, 2008). These results prompted us to investigate what transcriptomic changes were taking place in the embryos to be able to identify the mechanisms by which the plastic leachates were affecting development.

### 3.2. Identification of transcriptomic differences derived from PVC leachate exposure

To gain understanding of the functional genetic perturbations caused by exposure to microplastic leachates we compared genome-wide transcription profiles of animals exposed to PVC leachates with their non-exposed siblings. We focused on the PVC treated embryos for the interesting and clear aberrant phenotype observed, including an exogastrula with an apical outgrowth, and because we think there is a more likely possibility of finding higher concentrations of new particles, right after a spill, rather than drifted ones. We sequenced three biological replicates consisting of thousands of larvae each for 10 % PVC leachates and not-exposed siblings at 48 hpf (corresponding to late gastrula in the control) and 72 hpf (corresponding to pluteus larva in the control). The choice of the developmental stages analysed was based on the

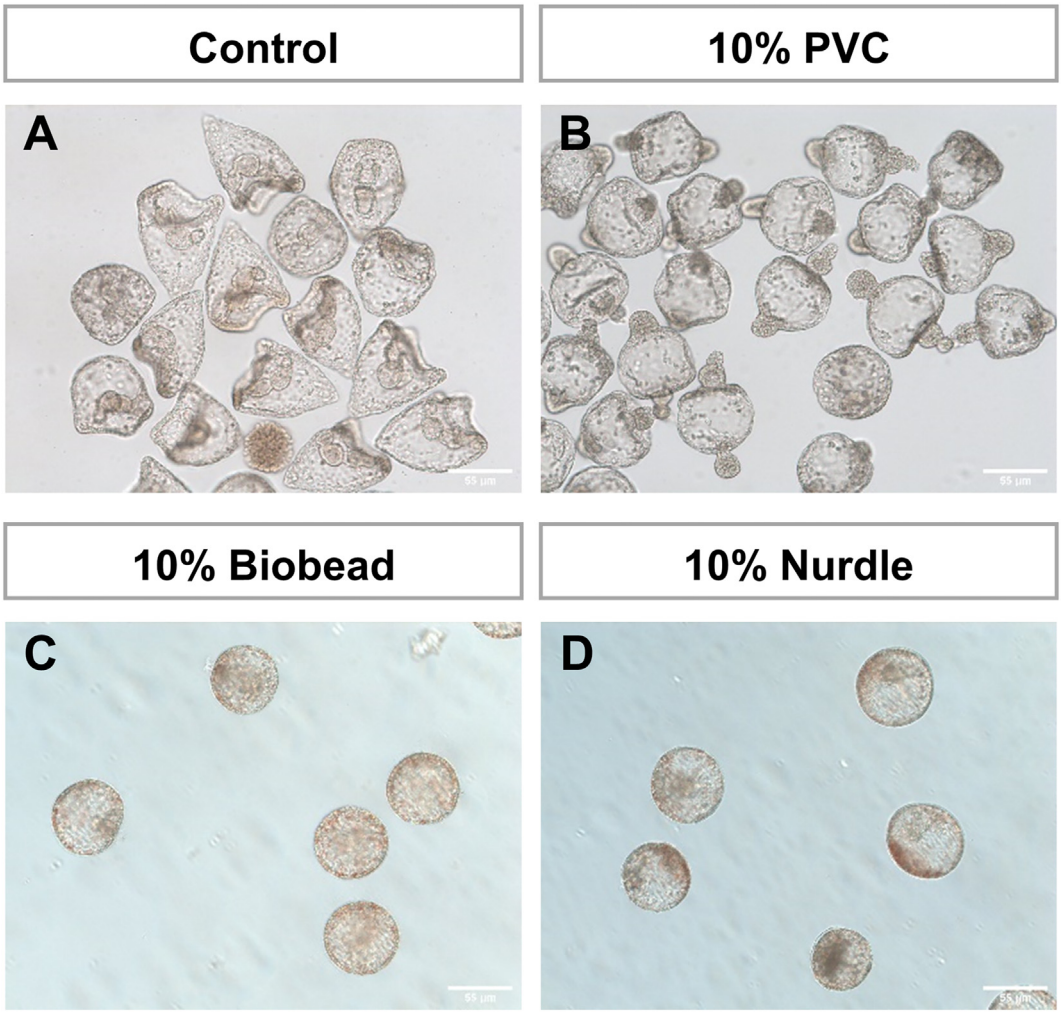


**Fig. 1.** Phenotypes of plastic leachate treated larvae. Phenotypic comparison of control and treatment *Strongylocentrotus purpuratus* larvae at 72 hpf. Treatments plastic leached for 72 h. PVC (B), Biobead (C) and Nurdle (D) leachates at 10 % particle concentrations (*v*/v). Scale bars are 55 μm.

fact that 48 hpf corresponds to the embryonic stage in which most of the cell fates have been sealed, while at 72 hpf larval free swimming and feeding lifestyle begins. The yield per sample ranged between 26 and 48 million paired-end 75-bp reads, with an average yield of 38.6 million reads per sample (Dobin et al., 2013; Liao et al., 2014; Kudtarkar and Cameron, 2017). Differential gene expression analysis was estimated DESeq2 (Love et al., 2014). PCA analysis showed distinct signatures for treated and control samples, as well for the two different stages (Fig. 3. A). A comprehensive list of differentially expressed genes is provided in Supplementary file 1. At 48 hpf, a total of 1590 were differentially expressed, using a log2fold-change of |1.5| or more and an adjusted *p*-value of <0.05. Of these, 219 were up-regulated and 1371 were down-regulated (Fig. 3. B, C). Using the same parameters, at 72 hpf, a total of 1929 genes were differentially expressed, 440 up-regulated and 1489 down-regulated (Fig. 3. B, D). In both stages, down-regulated genes represented >75 % of the differentially expressed genes (86 % at 48 hpf and 77 % at 72 hpf) suggesting that the effect by PVC leachates is of repressive nature, leading to a developmental program failure. At both time-points, the number of differentially expressed genes represents approximately 1/10 of the total amount of genes expressed by the end of *S. purpuratus* embryogenesis (Tu et al., 2014).

To analyse what type of processes are altered in the treated embryos we performed a gene ontology (GO) enrichment analysis using ShinyGO 0.76 platform (Ge et al., 2020) followed by REVIGO (Supek et al., 2011) to reduce redundant terms and visualise the data, separately for up- and down-regulated genes and each time point. We found several overrepresented GO terms at 48 h for both up- and down-regulated genes, broadly including: detection and response to stimuli, signaling pathways, development and developmental processes, metabolic and biosynthetic processes, regulation of processes and transport. At 72 hpf we find metabolic processes, regulation and development to be overrepresented in both up- and down-regulated genes. Moreover, for up-regulated genes we see response to external stimuli and cell organisation GO terms overrepresented, while for down-regulated genes we find signaling pathways and transport overrepresented (Supplementary Fig. S2).

To further characterise which cell types were most likely to be affected by the leachate treatment, we mapped the differentially expressed genes found in our transcriptomic data to single cell type atlases available for *S. purpuratus* (Paganos et al., 2021). We selected differentially expressed genes with log2fold-change of |1.5| or more and an adjusted *p*-value of <0.05, and scored their average expression across the cell type families in both developmental stages. According to the single cell analysis (Fig. 4), the majority of the downregulated genes at both developmental stages are enriched in ectodermally-derived cell types such as the anterior neuroectoderm/apical plate, aboral ectoderm and neurons, which is also in line with the morphological features of the treated larvae observed. Moreover, at both stages downregulated genes mapped to the immune cells (pigment and globular at 48 hpf), and skeletal cells. Surprisingly, no downregulated genes were found enriched in the endodermally derived cell types families at 48 hpf, despite the observed absence of a well-formed gut in the treated embryos, while at 72 hpf the anal and intestinal

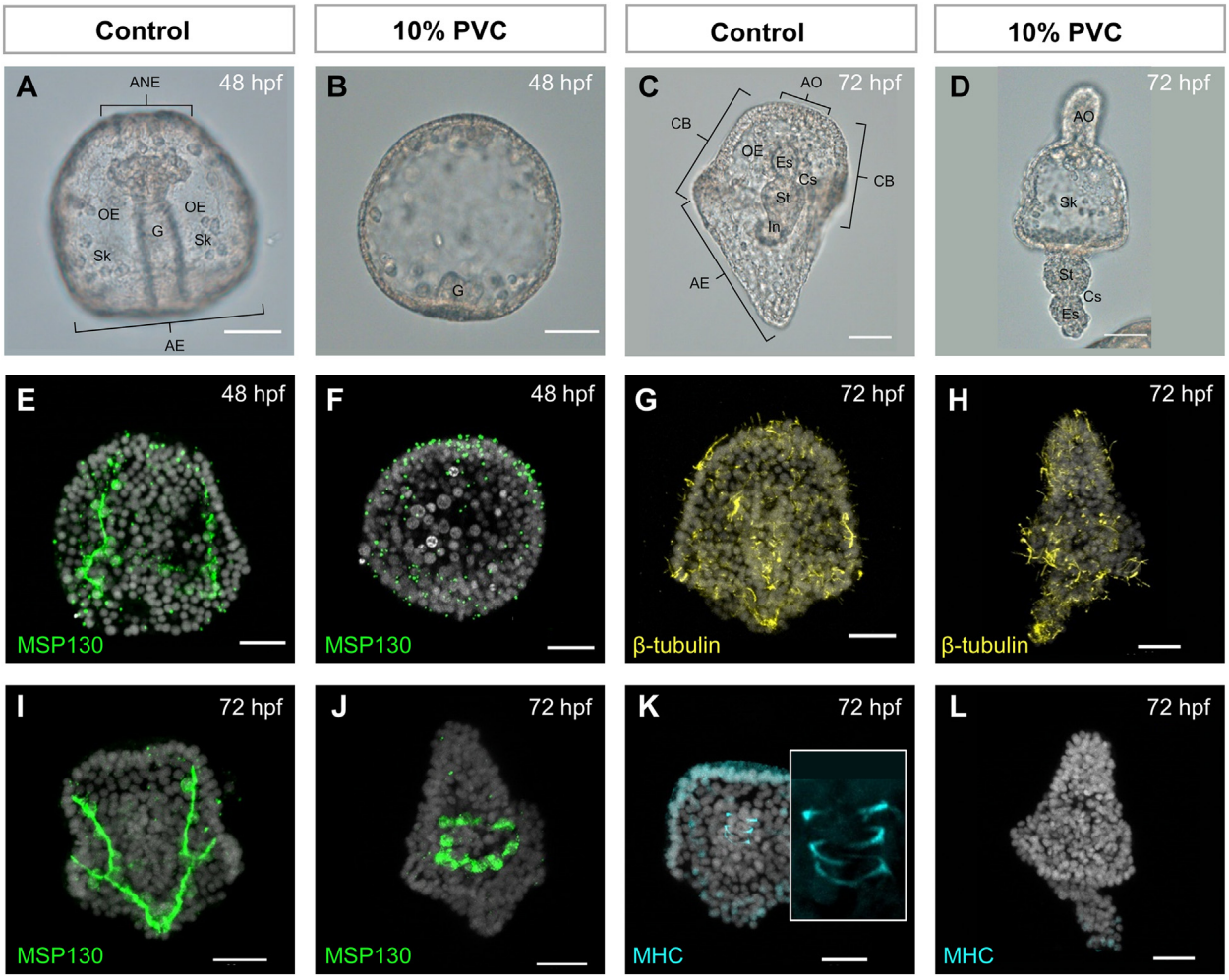


**Fig. 2.** Phenotypic characteristics of the PVC treated embryos and larvae. (A) Control 48 hpf gastrula embryo. (B) 48 hpf PVC treated embryo. (C) 72 hpf control pluteus larva. (D) 72 hpf PVC treated specimen. IHC detection of the skeletal marker Msp130 in (E, I) control and (F, J) PVC treated specimens. IHC detection of the cilia marker β-tubulin (G) in control and (H) PVC treated samples and of the muscle marker MHC in (K) control and (L) PVC treated samples. DAPI was used to visualise nuclei (grey). Scale bar is 36 μm. Inset in (K) shows a magnification of muscle staining. AE, Aboral ectoderm; ANE, Anterior neuroectoderm; AO, Apical Organ; CS, Cardiac sphincter; G, gut; In, Intestine; Es, Esophagus; OE, Oral Ectoderm; Sk, Skeletogenic cells; St, Stomach.

cell type families appear to contain target genes. On the contrary, an enrichment of upregulated genes in several endodermally-derived clusters is reported, suggesting that the malformation of the gut could be a result of gene upregulation rather than silencing. The enrichment of upregulated genes in the midgut and foregut domains appears to be conserved at the two developmental stages, as is the enrichment in the small micromeres/coelomic pouches and oral ectoderm domains. Overall, this comparison allowed us to verify the quality of our deRNA-seq data and analysis, as most of the deregulated genes are found in cell types that are clearly affected as judged by the specimens' morphology.

Next, we characterised in detail key genes that appear to be deregulated and are either part of cell type specification gene regulatory networks (GRNs) or markers of distinct cell types. In particular, based on the similarity of the PVC-obtained phenotype to the one obtained when the ectoderm of the embryo is oralised, we looked at members of the oral/aboral (OA) axis specification gene regulatory networks affected in our earliest timepoint (48 hpf), a stage in which the AO axis is specified in normal conditions. The oral/aboral axis in sea urchin is established at blastula stage through the action of the Tgfβ family members and especially *Nodal* and *Bmp2/4* as well as *Chordin* and *Lefty* (Molina et al., 2013). mRNAs of all four genes are expressed in the oral ectoderm organiser-like domain and are under the control of Nodal signaling, which is the main activator of the oral ectoderm gene regulatory network (Duboc et al., 2004, 2008; Bradham et al., 2009; Saudemont et al., 2010), while *Nodal* expression is controlled through a redox-sensitive mechanism (Nam et al., 2007). On the other hand, *Nodal* downstream targets *Bmp2/4* and *Bmp5/8* are transcribed in the oral ectoderm domain and through protein transport are activating the aboral ectoderm GRN (Ben-Tabou de-Leon et al., 2013). Lefty and Chordin proteins ensure that Nodal and Bmp2/4 signalings are restricted to the oral and aboral ectoderm respectively. In our transcriptomic data (summarised for the OA axis in Fig. 5) *Sp-Nodal*, *Sp-Chordin*, and *Sp-Lefty* are upregulated, indicative of ectoderm oralisation. Moreover, *Sp-Univin*, a known activator of Nodal as well as *Sp-Admp*, *Sp-Not*, *Sp-Gsc*, *Sp-Bra* and *Sp-FoxA*, all known members of the oral ectoderm GRN and whose expression is Nodal dependent, were found upregulated in our data. On the contrary, genes sitting on top of the GRN hierarchy including *Sp-Bmp5/8*, *Sp-Tbx2/3*, *Sp-Hox7*, *Sp-Msx*, *Sp-IrxA*, *Sp-Dlx* and *Sp-Hmx* are downregulated, suggesting that the aboral ectoderm is not specified in the PVC treated larvae. Indeed, FISH confirmed the ectopic expression of *Nodal*, and *Chordin* and *Bra* both at 48 and 72 hpf (Fig. 6. A1–A4, B1–B4, Supplementary Fig. S3. B, B′) as well as of the oral ectoderm marker *Sp-FoxABL* (Paganos et al., 2021) (Supplementary Fig. S3. A, A′). On the other hand, the ectoderm oralisation was validated by testing for the expression of genes normally found in the other two major ectodermal domains of ciliary band and aboral ectoderm. FISH for the ciliary band marker *Sp-Fbsl_2* (Paganos et al., 2021) shows accumulation of such

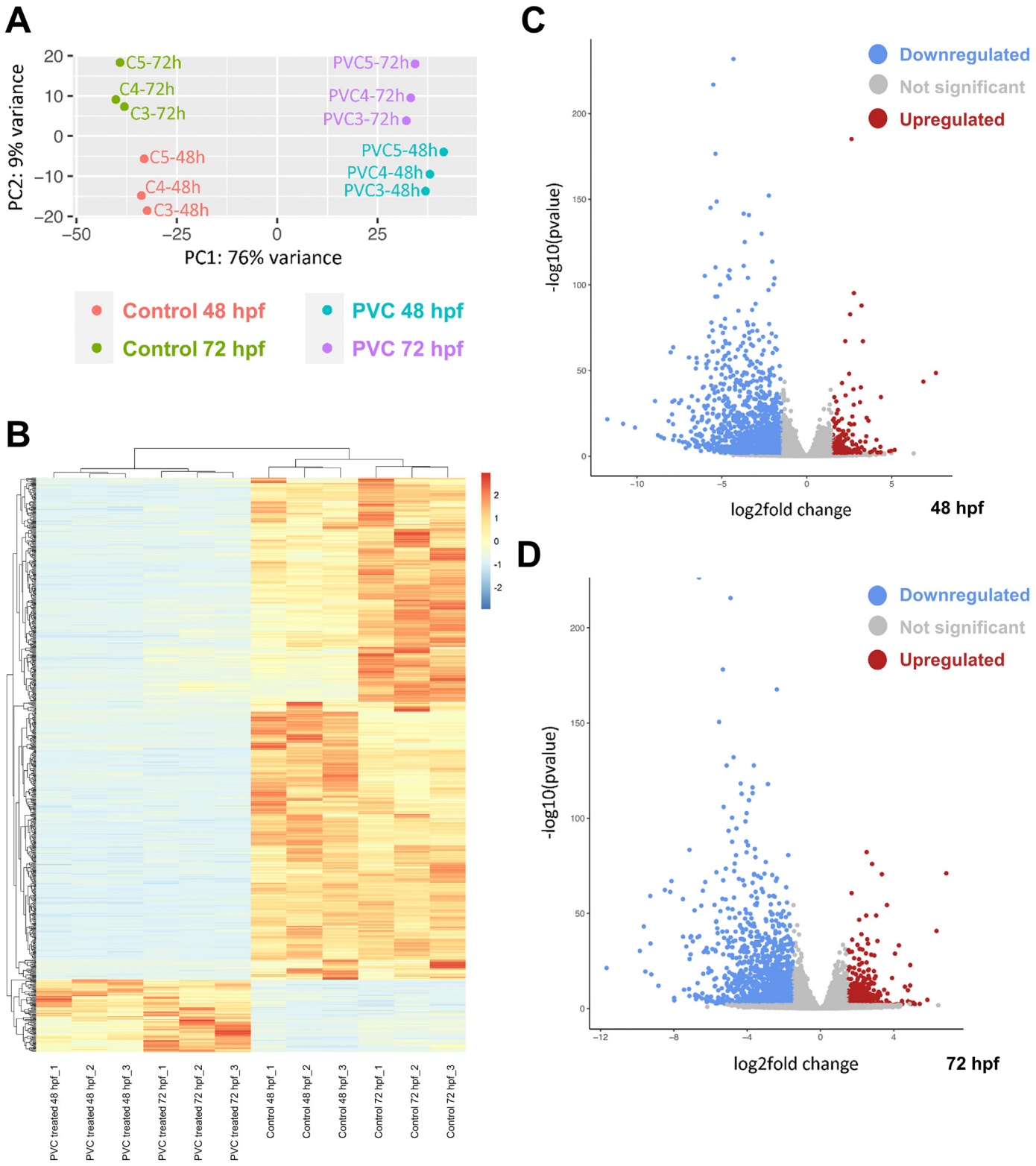


**Fig. 3.** Sample similarities and differential gene expression. (A) Principal component analysis plot of PVC treated and control samples at 48 and 72 hpf. Red: control treatment at 48 hpf; green: control treatment at 72 hpf; teal: PVC treatment at 48 hpf; magenta: PVC treatment at 72 hpf. (B) Heatmap of the normalised counts of each individual transcriptome corresponding to genes with log2fold change ($\geq|1.5|$) and that are simultaneously differentially expressed both at 48 hpf and 72 hpf. Blue is downregulated genes and red is upregulated genes. (C) 48 hpf and (D) 72 hpf volcano plots of down-regulated (blue) and up-regulated (red) genes at log2fold change $\geq|1.5|$ and adjusted *p*-values of <0.05. Grey is non-significant differentially expressed genes.

transcripts within the very well defined region of ciliary band, while PVC leachates treated specimens appear to be lacking it, with the exception of two ciliated patches found in the posterior part of the body closed to the gut (Fig. 6. A9, A10, B7, B8). Finally, the loss of the aboral ectoderm was confirmed by FISH for the aboral ectoderm marker *Sp-Spec1a* (Hardin et al., 1988) (Fig. 6. A7, A8, B3, B4).

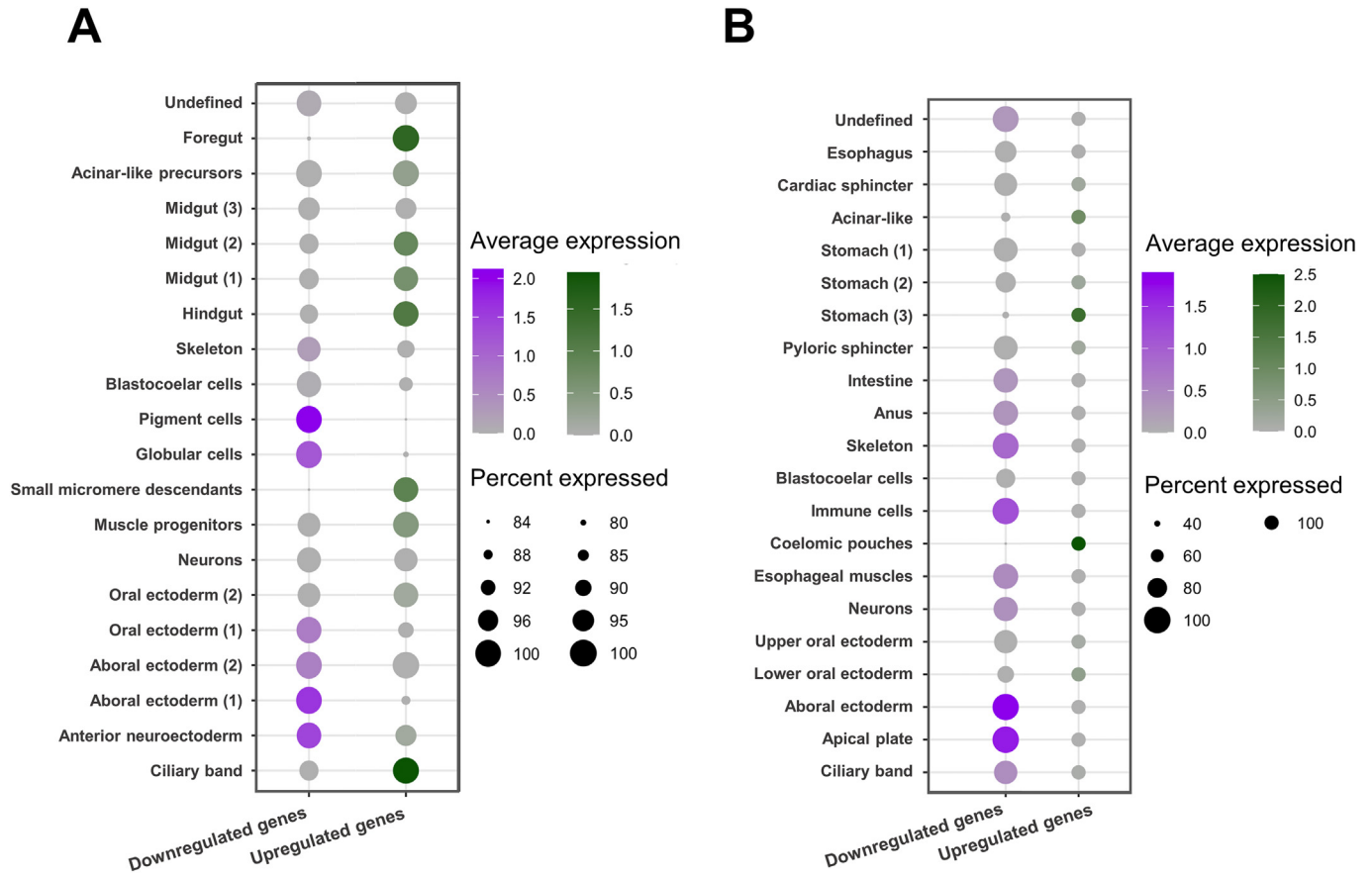


**Fig. 4.** Distribution of the deregulated genes across the embryonic and larval cell type families. Dotplot showing the average score of the downregulated (purple) and upregulated (green) genes after PVC treatment at (A) 48 and (B) 72 hpf.

According to our scRNA-seq analysis many of the deregulated genes at both developmental time-points are expressed by anterior neuroectoderm/apical plate, muscle, immune and skeletal cell type families. Further exploring our deRNA-seq data, we identified transcription factors related to the apical plate (Paganos et al., 2021) downregulated, such as *Sp-FoxJ1*, *Sp-Z167*, *Sp-Hbn*, *Sp-Ac/Sc*, *Sp-Emx*, *Sp-Mox*, *Sp-Rx*, *Sp-Pax6* and *Sp-Zic*, while *Sp-Otp* has been found to be expressed in larval prepancreatic neurons and to be involved in their differentiation (Slota and McClay, 2018; Paganos et al., 2021). It has been shown that downregulation of one or two of the apical plate transcription factors is sufficient for the malformation of serotonergic neurons. In line with our transcriptomic data, FISH for *Sp-Hbn*, *Sp-Pax6* and *Sp-Otp* validated their downregulation in treated specimens (Supplementary Fig. S3. D, D′, E, E′, L, L′). Furthermore, evidence of neuronal deficits is the downregulation of genes encoding for neurotransmitter, neuropeptides and synaptic machinery such as *Sp-Syt1*, *Sp-Chat*, *Sp-Salmfap*, *Sp-Tph*, *Sp-Th*, *Sp-An* and *Sp-Ngfffap*. FISH for the serotonergic neuron marker *Sp-Tph* both at 48 and 72 hpf verified the absence of Tph mRNAs in the treated specimen suggesting that serotonergic neurons are absent (Supplementary Fig. S3. C, C′, Q, Q′). In fact, FISH for sea urchin pan-neuronal marker *Sp-Syt1* (Burke et al., 2006) confirmed the absence of differentiated neurons in the PVC oralised larvae (Fig. 6. B5, B6), while the *Sp-SoxC* transcript, indicative of the presence of neuronal precursors, was found upregulated (Supplementary Fig. S3. S, S′).

Esophageal muscles and immune cells are two cell types consistently targeted by our PVC treatments across the development stages analysed. The ontogeny of both populations has been studied in great detail and it has been demonstrated that they arise from different partitions of the non-skeletogenic mesoderm; muscle progenitors from the oral and immune cells from the aboral mesoderm. Our transcriptomic analysis and FISH verified the loss of immune cells such as pigment cells. For instance, we find downregulation of *Sp-Gcm*, a gene necessary for the specification of pigment cells (Ransick and Davidson, 2006; Perillo et al., 2020), and *Sp-Pks1*, typically expressed in these cells (Griffiths, 1965), as well as other pigment cell markers (*Sp-Fmo2*, *3* and *5*, *Sp-Mif4* and 5), and downregulation of *Sp-MacpfA2*, a marker for globular cells (CH Ho et al., 2016). We confirm the absence of pigment cells by observing the downregulation of the *Sp-Pks1* gene at 48 and 72 hpf (Fig. 6. A5, A6, B9, B10). Regarding the muscle GRN, we find some of those genes only show expression divergences at 48 hpf. Interestingly, we report the downregulation of key transcription factors such as *Sp-ScratchX*, *Sp-Eya*, *Sp-FoxY*, *Sp-SoxE*, *Sp-Tbx6*, *Sp-FoxF*, *Sp-FoxL1*, *Sp-Six1/2*, all necessary for the specification of muscle progenitors (Andrikou et al., 2015). Finally, as demonstrated also by IHC Sp-MHC (Fig. 2. K, L), one of the terminal differentiation products of the aforementioned GRN (Andrikou et al., 2015), is also downregulated in the PVC treated larvae.

We also find that, while the ectodermal and mesodermal genetic programs appear to have been extensively rewired or even repurposed upon PVC treatment, the one operating in the endodermal cells is sufficient to form a partitioned, however mispatterned, digestive tract. FISH for the hindgut markers and downregulated genes in our differential analysis *Sp-Cdx1*, *Sp-Pdx1*, *Sp-Rhox3* (Cole and Arnone, 2009; Paganos et al., 2021) revealed the absence of such transcripts at 48 hpf treated embryos (Supplementary Fig. S3. H, H′, I, I′, J, J′) and a restricted expression domain at 72 hpf pluteus stage in regard to the controls (Supplementary Fig. S3 P, P′, T, T′). Moreover, the midgut marker domain *Sp-ManrC1a* revealed that the midgut/stomach domain is specified (Fig. 6. A11, A12, B11, B12), while FISH for *Sp-Ptf1a* and *Sp-Cpa2L* markers of the specialised for digestion acinar-like cells showed that, although less in number, acinar cells are specified (Supplementary Fig. S3. F, F′, R, R′). The reduction of the number of acinar-like cells is in line with the predicted downregulation of *Sp-*

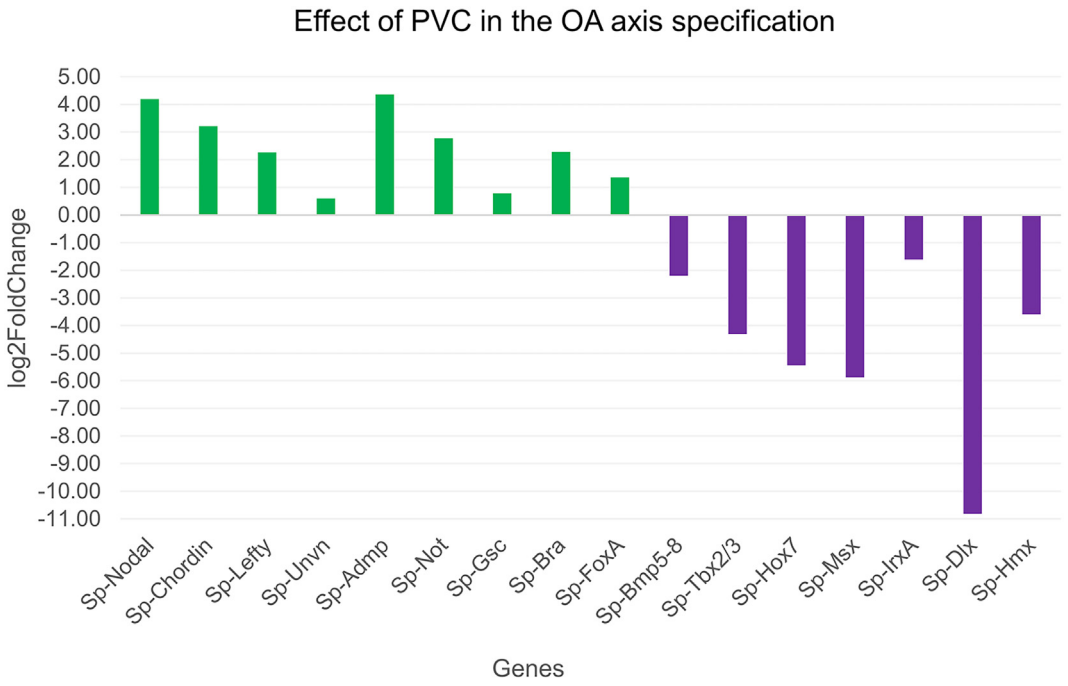


**Fig. 5.** PVC treatment disturbs genetic networks involved in oral aboral axis specification. Bar plot showing the upregulation (green) of the oral ectoderm GRN members and the downregulation (purple) of the aboral ectoderm GRN ones.

*Ptf1a*, the main driver of acinar-like cells specification (Perillo et al., 2016), validated by FISH (Supplementary Fig. S3. F, F′). Finally, we tested whether the expression of *Sp-Fgf9/16/20*, a gene with multiple roles during sea urchin development, is affected as predicted by the deRNA-seq analysis. At pluteus stage, *Sp-Fgf9/16/20* is normally expressed in the cardiac, pyloric and anal sphincter domains of the larva. Interestingly, in the PVC treated specimens at 72 hpf *Sp-Fgf9/16/20* expression is found in two band like domains at the two ends of the *Sp-ManrC1A* positive midgut region (Supplementary Fig. S3. O, O′) suggesting that pyloric and cardiac sphincters are partially formed. However, at 48 hpf gastrula stage, a stage in which this FGF ligand is involved in skeletogenesis, no transcripts were found in the treated embryos (Supplementary Fig. S3. G, G′), corroborating the differential analysis and the mispatterning of the skeleton shown by Msp130 IHC (Fig. 2. F and J). The mispatterning of the skeleton is also supported by the upregulation of the transcription factor *Sp-Ets1*, typically found in skeletogenic cells and sitting on top of the gene regulatory hierarchy, something also confirmed by FISH (Supplementary Fig. S3. K, K′, U, U′).

### 3.3. Identification of metabolic differences derived from PVC leachate exposure

To validate the surprisingly high number of metabolic pathways found affected in our functional gene enrichment analysis, we performed untargeted metabolomic analysis of our samples (Supplementary file 2). To assess metabolic alterations due to PVC treatment, we first analysed the basal physiological metabolism of embryos growth in normal conditions (Fig. S4. A). Hierarchical clustering obtained by fold change analysis (cut-off 2.0) in 72 hpf samples identified increased metabolic activity compared to the 48 hpf, as expected in normal embryo development (such as: nucleotides, aminosugars, amino acids, TCA cycle, unsaturated fatty acids and linoleic metabolism) (Fig. S4. A). At 48 hpf, the untargeted metabolic profile of PVC treated embryos showed seventy-three significant metabolites largely increased as compared to controls, essentially involved in lipid and fatty acids metabolism (Fig. S4. B). This increase in metabolites at early stages is seen in other animal models during embryonic development or under stress conditions to overcome a need to find new pathways to make energy (Wang et al., 2019, 2022). Rapid metabolic changes must occur in response to environmental changes to maintain redox and energetic homeostasis, survival and development (Koyama et al., 2020). However, the metabolic activation at 72 hpf seen in the controls was lost in embryos exposed to PVC leachates. Metabolic signatures showed eighty-one significant metabolites largely decreased at 72 hpf in PVC-leached treatment (Fig. S4. C). The enrichment analysis shows the profound impact of PVC treatments on a broad range of cellular metabolic pathways, including: nucleotides, amino sugars, glucose metabolism, fatty acids and redox metabolism as compared to controls (Fig. S4. C). This later metabolic decrease at 72 hpf could be related to the malformation of the gut, which is a large regulator of development of sea urchin larvae (Buckley et al., 2019; Fleming et al., 2021), or because the embryos have suffered such a catastrophic alteration that metabolic homeostasis cannot be achieved. In any case, from our results we suspect malfunction of the DNA/RNA synthesis program and decreased mitochondrial activity, by the observation of decreased levels of metabolites involved in nucleotides and increased redox stress (Fig. S4. C).

To gain a deeper understanding of the impact of PVC leachates in embryonic development, we performed targeted analysis looking into TCA cycle metabolites (Supplementary file 3). This shows decreased relative abundance of TCA cycle intermediates in PVC treated embryos both at 48 and 72 hpf, consistent with transcriptomic data (Fig. 7. A), and suggesting a failure in the mitochondrial ability to produce energy. The metabolic plasticity observed between 48 and 72 hpf in response to PVC leachate exposure suggests how metabolites might impact on the misregulated genes shown by the transcriptomic analysis. At 48 hpf, we find a faint correlation between the metabolic pathways affected and the misregulated genes (data not shown), that is potentially linked to the absence of the main metabolic and detoxification centre of the embryo: the archenteron (Fleming et al., 2021). Interestingly, based on the metabolomic and transcriptomic information of PVC treatments at 72 hpf, the metabolic pathways related to nucleotides metabolism (purine metabolism, pyrimidine metabolism and pentose phosphate pathway) are downregulated, as shown both at transcriptomic and metabolic level (Fig. 7. B), confirming problems in the synthesis of DNA and RNA. Moreover, the significantly decreased glutathione levels and its total conversion to the oxidised form in treated samples, as compared to control at 48 hpf, demonstrate high oxidative stress due to PVC exposure (Fig. 7. C). Furthermore, the GSH levels are restored at 72 hpf in PVC samples (Fig. 7. C), derived from the de novo synthesis (Fig. 7. D). All these suggest an attempt to recover the protection from

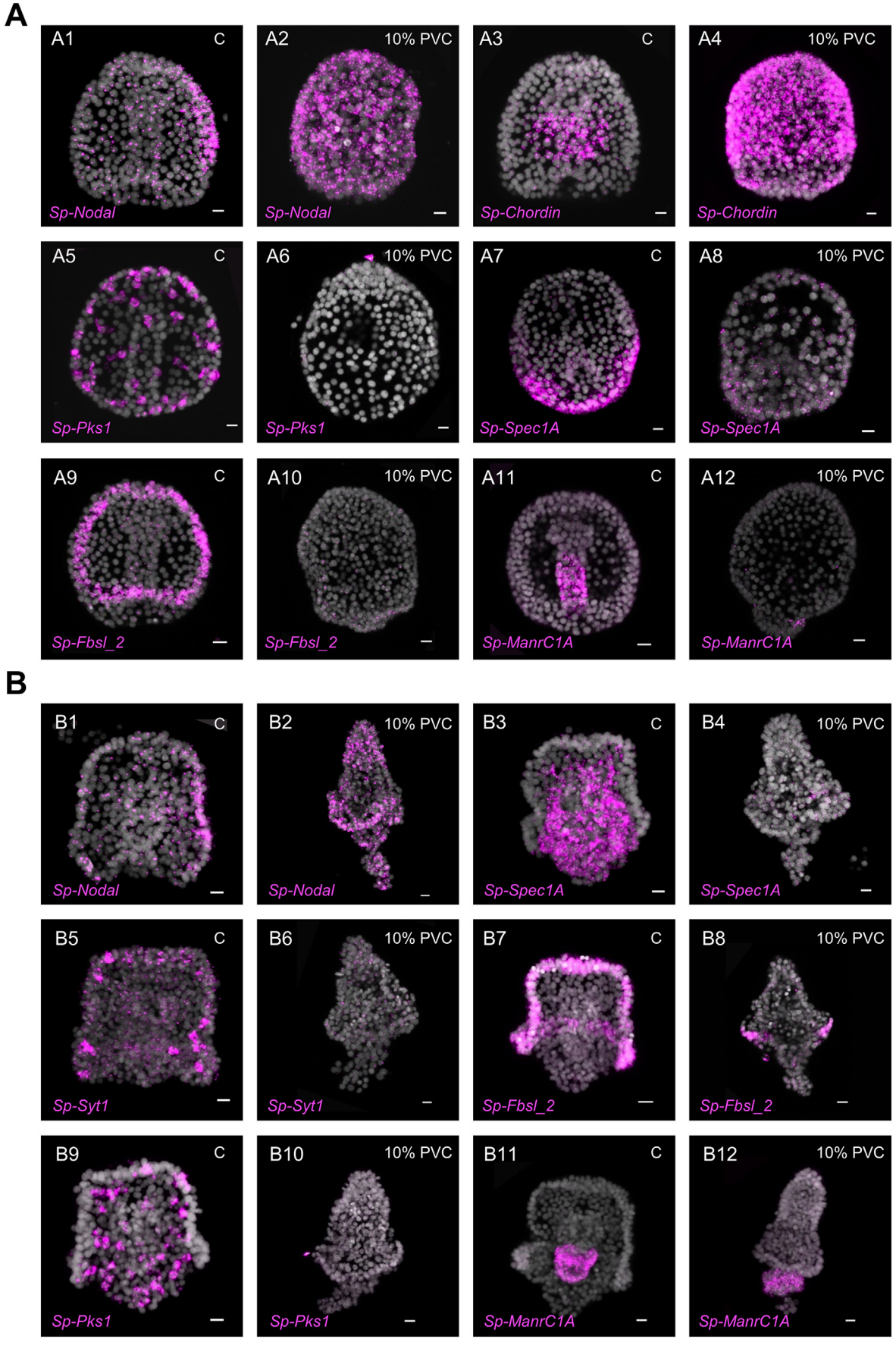
A
A1
C
Sp-Nodal
A2
10% PVC
Sp-Nodal
A3
C
Sp-Chordin
A4
10% PVC
Sp-Chordin
A5
C
Sp-Pks1
A6
10% PVC
Sp-Pks1
A7
C
Sp-Spec1A
A8
10% PVC
Sp-Spec1A
A9
C
Sp-Fbsl_2
A10
10% PVC
Sp-Fbsl_2
A11
C
Sp-ManrC1A
A12
10% PVC
Sp-ManrC1A
B
B1
C
Sp-Nodal
B2
10% PVC
Sp-Nodal
B3
C
Sp-Spec1A
B4
10% PVC
Sp-Spec1A
B5
C
Sp-Syt1
B6
10% PVC
Sp-Syt1
B7
C
Sp-Fbsl_2
B8
10% PVC
Sp-Fbsl_2
B9
C
Sp-Pks1
B10
10% PVC
Sp-Pks1
B11
C
Sp-ManrC1A
B12
10% PVC
Sp-ManrC1A

redox stress during abnormal development. Taken together, these results confirm how broad alteration in metabolism and in redox homeostasis due to PVC leachates contributes to abnormal embryo development.

### 3.4. Elemental analysis of microplastic water leachates

Following the observation of the phenotypes described, which are very similar to those found in the literature as caused by heavy metal exposure (Mitsunaga and Yasumasu, 1984; Hardin et al., 1992; Kobayashi and Okamura, 2004; Cunningham et al., 2020), we searched for metal detoxification pathways in the PVC-treated larval transcriptomes. Metallothioneins (MT) are heavy metal-induced proteins involved in the binding of metals for detoxification, transport and storage of those metals. *S. purpuratus* has three metallothioneins: *Sp-MTb1*, *Sp-MTb2* and *Sp-MTa* (Nemer et al., 1985; Ragusa et al., 2017). They are developmentally regulated and are induced by 2+ metal ions. Several reports show transcriptional activation of *MT* upon exposure to Zn: MT have been found to be overexpressed in the endomesodermal tissues of the pluteus larvae (Nemer et al., 1984) as well as ectopically expressed in all tissues of radialised embryos (Ragusa et al., 2017). In our transcriptome, we see upregulation of *MTa* at both 48 hpf and 72 hpf, being the second most overexpressed gene in both time points with a fold change of >115 at 48 hpf and 80 at 72 hpf. This finding points to an exposure to heavy metals in the embryos, which coincides with our hypothesis, derived from the comparison of the radialised/oralised phenotypes found here to phenotypes observed in sea urchin embryos treated with heavy metals in the literature (Mitsunaga and Yasumasu, 1984; Hardin et al., 1992; Kobayashi and Okamura, 2004; Cunningham et al., 2020). Given these insights we next set out to find possible metal contamination in the plastic leachates.

We determined the elements found in excess of the controls (Supplementary file 4) by inductively coupled plasma – optical emission spectrometry (ICP-OES) for all treatments used. We interrogated our samples for a set of relevant metals (see Materials and methods section) and found that only in the case of PVC pellets there is a significant increase in the presence of Zn, with solutions averaging 1.00 μg/g for Zn ($n$ = 4, range = 0.78 to 1.18 μg/g) in the 10 % PVC leachates, while in nurdles and biobeads the counts for Zn are below the limit of detection for the method, i.e. <~0.06 μg/g. Of the other tested heavy metals none could be substantiated in any of the processed samples other than Ba, which was persistently above levels of the seawater control sample in all PVC experiments (4200 to 5300 counts per second with respect to a maximum of 1300 in seawater). We observe a coupling with a slight increase in Ba and decrease in Sr in the samples with high concentration of Zn.

Plastic pellets, and in particular PVC, have chemicals other than the plastic polymer added to obtain desired characteristics of the plastics. Plasticisers, stabilisers and antifouling agents are necessary for obtaining a product fit for the production of plastic items. However, some of these additives are hazardous. An example of these are stabilisers, which improve the resistance of the plastics as well as facilitate the processing of the nurdles into a final product. Calcium based stabilisers are regularly used in the production of PVC and other plastic pellets. These include calcium, zinc, heat stabilisers, and they are deemed safe by legislation in Europe, Canada and the USA (European Stabiliser Producers Association). It is therefore not surprising to find Zn in these particles. Some liquid stabilisers can use Zn-Ba mixed metals, possibly explaining the slight increase in Ba in the PVC samples. We have demonstrated that this Zn can be leached into seawater from the PVC nurdles in laboratory conditions. We find a concentration of 1μg/g of Zn in 10 % leachates which cause an extreme abnormal phenotype. At lower PVC concentrations down to 1 %, corresponding to a concentration of Zn of 100 ng/g, animals do not develop properly either (Supplementary Fig. S1), and never reach a viable larva. We did not find an excess of other metals used as stabilisers such as Sn, Ph or Cd (now phased out) in our samples. The lack of Zn or other metals in our environmental samples indicates that the phenotype they elicit is not due to their metal content. However, in previous studies we have shown that they are capable of releasing persistent organic pollutants (Rendell-Bhatti et al., 2020) and these are most likely the cause of their toxicity here too. Hence, plastic nurdles have the capacity to be harmful twice: once, when first lost at sea because of the additives they contain, like we show here, and then as they collect (Mato et al., 2001; Ogata et al., 2009) and later release environmental pollutants from the water, as we showed before (Rendell-Bhatti et al., 2020).

### 3.5. Correlating plastic derived pollutants, heavy metals and sea urchin embryo development

Here we report PVC leachate-treated embryos show a radialised phenotype. The radialised phenotype has been previously described in the literature as a perturbation of the organisation of the oral aboral as well as the left/right axes of the embryo (Duboc et al., 2004). In fact, the gene *Nodal* is known to be responsible for this organisation (reviewed in (Molina et al., 2013)). *Nodal* is expressed very early in the presumptive oral ectoderm, and overexpression of this gene transforms the whole ectoderm into oral ectoderm, inducing as well ectopic expression of orally expressed genes (Duboc et al., 2004). The oralisation of the embryo comes at the expense of other structures. In the case of *Nodal* overexpression, it is known that these embryos lack pigment cells (Duboc et al., 2010). High doses of *Nodal* are known to block the formation of the skeleton, while low doses allow the formation of a radialised skeleton (Mcintyre et al., 2014). *Nodal* overexpression is also known to generate the absence of serotonergic neurons in the anterior neuroectoderm (McClay et al., 2018). Our transcriptomic data, also confirmed by FISH, shows an overexpression of *Nodal* in our embryos, which also show the loss of structures and cell types linked to increased Nodal levels.

It is known that exposure of early sea urchin embryos to heavy metals produces abnormal phenotype larvae (Mitsunaga and Yasumasu, 1984; Hardin et al., 1992; Duboc et al., 2004; Kobayashi and Okamura, 2004). Hardin et al. (1992) reported radialised pluteus when treated with $NiCl_2$, while Kobayashi and Okamura (2004) and Mitsunaga and Yasumasu (1984) showed radialised exogastrulae when embryos were treated with Zn. In fact, the link between heavy metal induced radialised phenotypes and *Nodal* overexpression was already drawn by Duboc et al. (2004). They found that $NiCl_2$ treatment caused overexpression of *Nodal* in a belt of cells around the embryo at the blastula stage (Duboc et al., 2004). In our study, matching the phenotypes observed, we see a downregulation of genes involved in the aboral and dorsal specification of the animal (Fig. 5). Interestingly, RNAseq analysis of sea urchin embryos exposed to Zn revealed similar upregulation of the oral ectoderm GRN members *Nodal*, *Chordin*, *Lefty* and *Gsc* and the downregulation of the aboral ectoderm GRN components *Tbx2/3*, *Msx* and *Spec1a* (Ertl et al., 2011). We also observe the downregulation of differentiation genes for the skeleton (Fig. 2. E, F, I, J), immune cells (Fig. 6. A5, A6, B9, B10) and neurons (Fig. 6. B5, B6), as well as an upregulation of genes responsible for the oralisation of the animal (Fig. 5). We see an overexpression of *Nodal* at both stages (Fig. 6. A1, A2, B1, B2), that explain the misspecification of both OA and LR axes we see in our larvae, with the oralisation of the ectoderm, the radialised skeleton and the absence of differentiated neurons, as well as the lack of pigment cells. The mechanisms by which heavy metals, and in our case Zn, affect gene expression is unknown, but here it seems clear that it is the response to heavy metals leached from the plastic

**Fig. 6.** In situ validation of the deRNA-seq predicted gene targets. (A) FISH using antisense probes for *Sp-Nodal*, *Sp-Chordin*, *Sp-Pks1*, *Sp-Spec1a*, *Sp-Fbsl_2* and *Sp-ManrC1A* at 48 hpf, in control (A1, A3, A5, A7, A9, A11) and PVC treated specimens (A2, A4, A6, A8, A10, A12), respectively. (B) FISH using antisense probes for *Sp-Nodal*, *Sp-Spec1A*, *Sp-Syt1*, *Sp-Fbsl_2*, *Sp-Pks1* and *Sp-ManrC1A* at 72 hpf, in control (B1, B3, B5, B7, B9, B11) and PVC treated specimens (B2, B4, B6, B8, B10, B12), respectively. DAPI was used to visualise nuclei (grey). Scale bars are 15 μm.

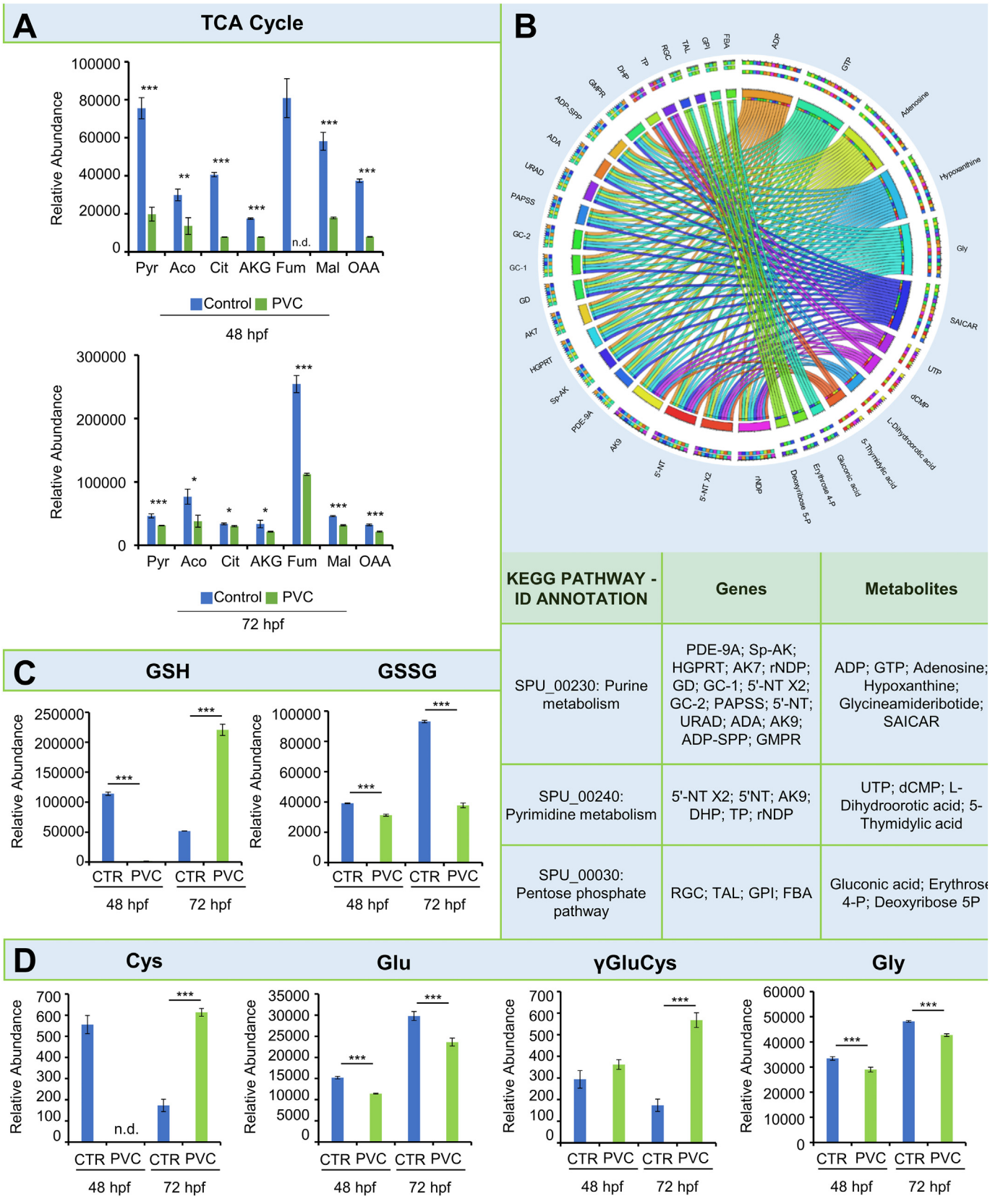


| KEGG PATHWAY - ID ANNOTATION | Genes | Metabolites |
|---|---|---|
| SPU_00230: Purine metabolism | PDE-9A; Sp-AK; HGPRT; AK7; rNDP; GD; GC-1; 5'-NT X2; GC-2; PAPSS; 5'-NT; URAD; ADA; AK9; ADP-SPP; GMPR | ADP; GTP; Adenosine; Hypoxanthine; Glycineamideribotide; SAICAR |
| SPU_00240: Pyrimidine metabolism | 5'-NT X2; 5'NT; AK9; DHP; TP; rNDP | UTP; dCMP; L-Dihydroorotic acid; 5-Thymidylic acid |
| SPU_00030: Pentose phosphate pathway | RGC; TAL; GPI; FBA | Gluconic acid; Erythrose 4-P; Deoxyribose 5P |

**Fig. 7.** Metabolic characterization in PVC treated specimens. (A) Relative abundance of TCA cycle metabolites at 48 hours post fertilisation (hpf) (left panel) and 72 hpf (right panel) in control and PVC exposed embryos ($n = 3$). (B) Circos plot (top panel) and relative table (bottom panel) showing significantly downregulated metabolites-genes at 72 hpf under PVC exposure within the same KEGG metabolic pathways. (C) Relative abundance of GSH (left panel), GSSG (right panel) and (D) glutathione synthesis intermediates at 48 hpf and 72 hpf in control and PVC exposed embryos (n = 3). Error bars indicate SD. *$p \leq 0.05$, **$p \leq 0.01$. ***$p \leq 0.005$.

particles that is generating the transcriptional dysregulation responsible for the phenotypes observed. It has been previously demonstrated that Zn affects the later phase of *Nodal* expression (feedback phase) rather than the initial one (initiation phase) (Ertl et al., 2011). However, our data suggest that PVC leachates induce high levels of oxidative stress. Several stressors such as UVB irradiation or X-rays result in similar skeleton malformations in sea urchins, while also generating oxidative stress (Bonaventura et al., 2005; Matranga et al., 2010). Heavy metal poisoning has been shown to cause mitochondrial damage affecting the cell capacity to cope with oxidative stress (Sun et al., 2022), and to induce oxidative stress in several species (Kim et al., 2014; Chiarelli et al., 2019). Indeed, our metabolic profiling shows decreased relative abundance of TCA cycle intermediates suggesting mitochondrial failure, as well as increased oxidative stress. Moreover, exposure to zinc induces an overexpression of metallothionein genes (Nemer et al., 1984), similar to what is observed in our transcriptomic data. At the same time, excess doses of zinc have been shown to decrease glutathione levels, and increase the oxidised/reduced ratio (Walther et al., 2008), as we observe in our 48 hpf metabolic analysis. The recovery and overproduction of reduced glutathione (GSH) levels in PVC treated larvae at 72 hpf suggests an upregulation of detoxification mechanisms, as demonstrated in other systems as an adaptation to zinc exposure (Qu et al., 2014). GSH has been found to inhibit Zn release from metallothioneins, stabilizing them at high cellular concentrations of GSH (Ruttkay-Nedecky et al., 2013), and increased glutathione synthesis has been shown to be able to decrease zinc mediated toxicity in human cell types (Walther et al., 2008). Hence, the overexpression of metallothioneins and overproduction of GSH at 72 hpf could be triggering oxidative stress recovery by the subsequent depletion of Zn in the larvae. Taken together, we hypothesise that either the PVC-related oxidative stress, probably caused by Zn exposure, is controlling the redox-sensitive expression of *Nodal* during the initiation phase, or that Zn overactivates the *Nodal* feedback loop mechanism, resulting in embryo radialisation. As a counteracting mechanism, metallothioneins are overproduced in an attempt to deplete toxic zinc in the larvae and to rescue embryonic development. With our morphological observations and mapping our transcriptomic data to single cell transcriptomic data available for *S. purpuratus* (Paganos et al., 2021) we have shown that PVC leachates-treated gastrulae mainly consist of oral ectoderm and a partially invaginated gut (Fig. 8.), while at 72 hpf most of the larva is still oral ectoderm, with no aboral or apical structures, no differentiated neurons, muscles or immune cells and only two patches of ciliated cells in regards to the wild type. They have however been able to form a small radial skeleton, and despite it having formed outside the body cavity, the gut seems to be tripartite and with the correct, although mispatterned, cell types (Fig. 8.).

Using a multi-omics approach we have been able to decipher the molecular mechanisms involved in the toxicity of PVC leachates in the sea urchin embryo, as well as a readout of the cellular processes that have been affected. We have defined which developmental gene pathways are disturbed and how they cause the phenotypic disturbances we have observed, and we have been able to pinpoint cellular redox stress as well as energy production as the cellular problems derived from the exposure to PVC leachates. Being able to provide a mechanistic understanding of the effect of plastic contamination is a great step forward in the way we approach this type of research. We believe that molecular work with deep and organismal-wide information like the one provided here is of great importance to advance our understanding of the consequences of how plastic pollution affects life.

## 4. Conclusions

Nurdle spills are, sadly, a source of unwanted plastic contamination, where enormous quantities of plastic nurdles can be found (Partow et al., 2021; Sewwandi et al., 2022). It is very unlikely that high concentrations of plastic pellets like the ones used in our study are found in environmental settings other than in some areas immediately after these accidents. Marine invertebrate development is a particularly sensitive life stage as it happens very quickly and directly in the water. We have shown that new plastic

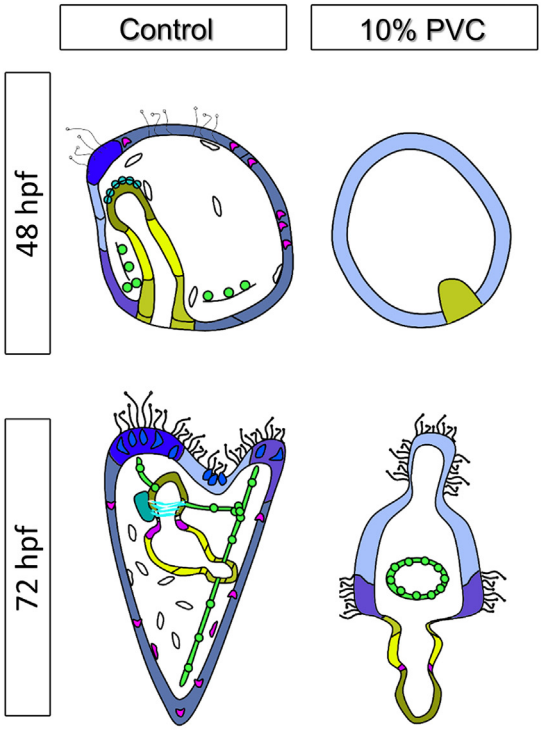


| Cell type family | Effect |
|---|---|
| Oral ectoderm | Expanded |
| Aboral ectoderm | Absent |
| Ciliary band | Mispatterned |
| Apical ectoderm | Absent |
| Neurons | Absent |
| Coelomic pouch | Absent |
| Immune cells | Absent |
| Skeleton | Mispatterned |
| Muscles | Absent |
| Esophagus | Mispatterned |
| Acinar-like | Mispatterned |
| Stomach/midgut | Mispatterned |
| Posterior gut | Mispatterned |

**Fig. 8.** PVC leachate-induced malformations in sea urchin embryos and larvae. Schematic representations showing the morphological and cell type phenotypic effects of PVC treatments at 48 and 72 hpf vs the controls as indicated by the present study. The effect on different cell family types is described in the table.

nurdles are able leach harmful chemicals, in particular heavy metals that, at high concentrations, disrupt the development of sea urchin embryos. These chemicals produce transcriptomic changes that involve the disruption of major developmental gene regulatory networks as well as metabolic pathways, and challenge axis formation and cell type specification and differentiation in sea urchin larvae. Given the highly conserved nature of developmental processes, it is not difficult to imagine that other organisms will also be affected in a similar way.

Supplementary data to this article can be found online at https://doi.org/10.1016/j.scitotenv.2022.160901.

## CRediT authorship contribution statement

**Periklis Paganos:** Conceptualization, Methodology, Validation, Formal Analysis, Investigation, Writing – Later draft, Review and editing, Visualisation

**Clemens V Ullman:** Methodology, Validation, Formal Analysis, Investigation, Resources, Writing – Review and Editing

**Daniela Gaglio:** Methodology, Formal Analysis, Resources, Writing – Review and Editing, Visualisation, Supervision

**Marcella Bonanomi:** Investigation, Writing – Review and Editing

**Noemi Salmistraro:** Investigation, Writing – Review and Editing

**Maria Ina Arnone:** Conceptualization, Resources, Writing - Review and Editing, Supervision

**Eva Jimenez Guri:** Conceptualization, Methodology, Validation, Formal Analysis, Investigation, Resources, Writing – Original Draft, Later draft, Review and editing, Visualisation, Supervision, Project Administration, Funding acquisition

## Data availability

Data will be made available on request.

## Declaration of competing interest

The authors declare that they have no known competing financial interests or personal relationships that could have appeared to influence the work reported in this paper.

## Acknowledgements

We would like to thank Emily Stevenson, from Beach Guardian CIC, for collecting materials at the beach and Tim Hammond for help with exporting PVC nurdles, Ricard Albalat and Loli Molina for helpful discussions, Karl R. Wotton for help with the transcriptomic data and GO enrichment analysis and critical reading of the manuscript, Davide Caramiello at SZN for animal maintenance and Erica Riccio for her valuable help in obtaining gametes. We would like to thank three anonymous reviewers for their constructive comments.

## Funding

PP has been supported by a Research Grant from the Human Frontiers Science Program (Ref.-No:RGP0002/2019 to MIA). EJ-G was supported, and the project was funded, by the European Union's Horizon 2020 research and innovation program under the Marie Skłodowska-Curie grant agreement no. 882904.

## References

Andrew Cameron, R., Davidson, E.H., 1991. Cell type specification during sea urchin development. Trends Genet. 7, 212–218. https://doi.org/10.1016/0168-9525(91)90367-Y.

Andrikou, C., Iovene, E., Rizzo, F., Oliveri, P., Arnone, M.I., 2013. Myogenesis in the sea urchin embryo: the molecular fingerprint of the myoblast precursors. EvoDevo 4, 33. https://doi.org/10.1186/2041-9139-4-33.

Andrikou, C., Pai, C.-Y., Su, Y.-H., Arnone, M.I., 2015. Logics and properties of a genetic regulatory program that drives embryonic muscle development in an echinoderm. eLife 4, 1–22. https://doi.org/10.7554/elife.07343.

Angerer, R.C., Davidson, E.H., 1984. Molecular indices of cell lineage specification in sea urchin embryos. Science 226, 1153–1160. https://doi.org/10.1126/science.6594757.

Annunziata, R., Arnone, M.I., 2014. A dynamic regulatory network explains ParaHox gene control of gut patterning in the sea urchin. Development 141, 2462–2472. https://doi.org/10.1242/dev.105775.

Arnone, M.I., Andrikou, C., Annunziata, R., 2016. Echinoderm systems for gene regulatory studies in evolution and development. Curr.Opin.Genet.Dev. 39, 129–137. https://doi.org/10.1016/j.gde.2016.05.027.

Arshinoff, B.I., Cary, G.A., Karimi, K., Foley, S., Agalakov, S., Delgado, F., Lotay, V.S., Ku, C.J., Pells, T.J., Beatman, T.R., Kim, E., Cameron, R.A., Vize, P.D., Telmer, C.A., Croce, J.C., Ettensohn, C.A., Hinman, V.F., 2022. Echinobase: leveraging an extant model organism database to build a knowledgebase supporting research on the genomics and biology of echinoderms. Nucleic Acids Res. 50, D970–D979. https://doi.org/10.1093/nar/gkab1005.

Ben-Tabou de-Leon, S., Su, Y.H., Lin, K.T., Li, E., Davidson, E.H., 2013. Gene regulatory control in the sea urchin aboral ectoderm: spatial initiation, signaling inputs, and cell fate lockdown. Dev. Biol. 374, 245–254. https://doi.org/10.1016/j.ydbio.2012.11.013.

Bonanomi, M., Salmistraro, N., Fiscon, G., Conte, F., Paci, P., Bravatà, V., Forte, G.I., Volpari, T., Scorza, M., Mastroianni, F., D'Errico, S., Avolio, E., Piccialli, G., Colangelo, A.M., Vanoni, M., Gaglio, D., Alberghina, L., 2021. Transcriptomics and metabolomics integration reveals redox-dependent metabolic rewiring in breast cancer cells. Cancers 13, 5058. https://doi.org/10.3390/cancers13205058.

Bonaventura, R., Poma, V., Costa, C., Matranga, V., 2005. UVB radiation prevents skeleton growth and stimulates the expression of stress markers in sea urchin embryos. Biochem. Biophys. Res. Commun. 328, 150–157. https://doi.org/10.1016/j.bbrc.2004.12.161.

Boucher, J., Friot, D., 2017. Primary microplastics in the oceans: A global evaluation of sources. IUCN International Union for Conservation of Nature https://doi.org/10.2305/IUCN.CH.2017.01.en.

Bradham, C.A., Oikonomou, C., Kühn, A., Core, A.B., Modell, J.W., McClay, D.R., Poustka, A.J., 2009. Chordin is required for neural but not axial development in sea urchin embryos. Dev. Biol. 328, 221–233. https://doi.org/10.1016/j.ydbio.2009.01.027.

Buckley, K.M., Schuh, N.W., Heyland, A., Rast, J.P., 2019. Chapter 14 - analysis of immune response in the sea urchin larva. In: Foltz, K.R., Hamdoun ABT-M in CB (Eds.), Echinoderms, Part A. Academic Press, pp. 333–355. https://doi.org/10.1016/bs.mcb.2018.10.009.

Burke, R.D., Osborne, L., Wang, D., Murabe, N., Yaguchi, S., Nakajima, Y., 2006. Neuron-specific expression of a synaptotagmin gene in the sea urchinStrongylocentrotus purpuratus. J. Comp. Neurol. 496, 244–251. https://doi.org/10.1002/cne.20939.

Carpenter, E.J., Anderson, S.J., Harvey, G.R., Miklas, H.P., Peck, B.B., 1972. Polystyrene spherules in coastal waterspolystyrene spherules in coastal waters. Science 178, 750–753. https://doi.org/10.1126/science.178.4062.750.

Carpenter, E.J., Smith, K.L., 1972. Plastics on the Sargasso sea surface. Sciences 175, 1240–1241. https://doi.org/10.1126/science.175.4027.1240.

CH Ho, E., Buckley, K.M., Schrankel, C.S., Schuh, N.W., Hibino, T., Solek, C.M., Bae, K., Wang, G., Rast, J.P., 2016. Perturbation of gut bacteria induces a coordinated cellular immune response in the purple sea urchin larva. Immunol. Cell Biol. 94, 861–874. https://doi.org/10.1038/icb.2016.51.

Chiarelli, R., Martino, C., Roccheri, M.C., 2019. Cadmium stress effects indicating marine pollution in different species of sea urchin employed as environmental bioindicators. Cell Stress Chaperones 24, 675–687. https://doi.org/10.1007/s12192-019-01010-1.

Cole, A.G., Arnone, M.I., 2009. Fluorescent in situ hybridization reveals multiple expression domains for SpBrn1/2/4 and identifies a unique ectodermal cell type that co-expresses the ParaHox gene SpLox. Gene Expr. Patterns 9, 324–328. https://doi.org/10.1016/j.gep.2009.02.005.

Cole, G., Sherrington, C., 2016. Study to quantify pellet emissions in the UK. Bristol, UK, Eunomia.

Cunningham, B., Torres-Duarte, C., Cherr, G., Adams, N., 2020. Effects of three zinc-containing sunscreens on development of purple sea urchin (Strongylocentrotus purpuratus) embryos. Aquat. Toxicol. 218, 105355. https://doi.org/10.1016/j.aquatox.2019.105355.

Dobin, A., Davis, C.A., Schlesinger, F., Drenkow, J., Zaleski, C., Jha, S., Batut, P., Chaisson, M., Gingeras, T.R., 2013. STAR: ultrafast universal RNA-seq aligner. Bioinformatics 29, 15–21. https://doi.org/10.1093/bioinformatics/bts635.

Duboc, V., Lapraz, F., Besnardeau, L., Lepage, T., 2008. Lefty acts as an essential modulator of nodal activity during sea urchin oral-aboral axis formation. Dev. Biol. 320, 49–59. https://doi.org/10.1016/j.ydbio.2008.04.012.

Duboc, V., Lapraz, F., Saudemont, A., Bessodes, N., Mekpoh, F., Haillot, E., Quirin, M., Lepage, T., 2010. Nodal and BMP2/4 pattern the mesoderm and endoderm during development of the sea urchin embryo. Development 137, 223–235. https://doi.org/10.1242/dev.042531.

Duboc, V., Röttinger, E., Besnardeau, L., Lepage, T., 2004. Nodal and BMP2/4 signaling organizes the oral-aboral axis of the sea urchin embryo. Dev. Cell 6, 397–410.

Engler, R.E., 2012. The complex interaction between marine debris and toxic chemicals in the ocean. Environ.Sci.Technol. 46, 12302–12315. https://doi.org/10.1021/es3027105.

Eriksen, M., Lebreton, L.C.M., Carson, H.S., Thiel, M., Moore, C.J., Borerro, J.C., Galgani, F., Ryan, P.G., Reisser, J., 2014. Plastic pollution in the world's oceans: more than 5 trillion plastic pieces weighing over 250,000 tons afloat at sea. PLoS ONE 9, 1–15. https://doi.org/10.1371/journal.pone.0111913.

Ernst, S.G., 2011. Offerings from an urchin. Dev. Biol. 358, 285–294. https://doi.org/10.1016/j.ydbio.2011.06.021.

Ertl, R.P., Robertson, A.J., Saunders, D., Coffman, J.A., 2011. Nodal-mediated epigenesis requires dynamin-mediated endocytosis. Dev. Dyn. 240, 704–711. https://doi.org/10.1002/dvdy.22557.

Essel, R., Engel, L., Carus, M., 2015. 64 /2015 Sources of Microplastics Relevant to Marine Protection in Germany.

Ettensohn, C.A., 2020. The gene regulatory control of sea urchin gastrulation. Mech. Dev. 162, 103599. https://doi.org/10.1016/j.mod.2020.103599.
European Stabiliser Producers Association, PVC stabilisers https://www.stabilisers.eu/stabilisers/.
Fleming, T.J., Schrankel, C.S., Vyas, H., Rosenblatt, H.D., Hamdoun, A., 2021. CRISPR/Cas9 mutagenesis reveals a role for ABCB1 in gut immune responses to vibrio diazotrophicus in sea urchin larvae. J. Exp. Biol. 224, jeb232272. https://doi.org/10.1242/jeb.232272.
Gardon, T., Huvet, A., Paul-Pont, I., Cassone, A., Koua, M.S., Soyez, C., Jezequel, R., Receveur, J., Le Moullac, G., 2020. Toxic effects of leachates from plastic pearl-farming gear on embryo-larval development in the pearl oyster Pinctada margaritifera. Water Res. 115890. https://doi.org/10.1016/j.watres.2020.115890.
Gauquie, J., Devriese, L., Robbens, J., De Witte, B., 2015. A qualitative screening and quantitative measurement of organic contaminants on different types of marine plastic debris. Chemosphere 138, 348–356. https://doi.org/10.1016/j.chemosphere.2015.06.029.
Ge, S.X., Jung, D., Yao, R., 2020. ShinyGO: a graphical gene-set enrichment tool for animals and plants. Bioinformatics 36, 2628–2629. https://doi.org/10.1093/bioinformatics/btz931.
Griffiths, M., 1965. A study of the synthesis of naphthaquinone pigments by the larvae of two species of sea urchins and their reciprocal hybrids. Dev. Biol. 11, 433–447. https://doi.org/10.1016/0012-1606(65)90049-7.
Hao, Y., Hao, S., Andersen-Nissen, E., Mauck III, W.M., Zheng, S., Butler, A., Lee, M.J., Wilk, A.J., Darby, C., Zager, M., Hoffman, P., Stoeckius, M., Papalexi, E., Mimitou, E.P., Jain, J., Srivastava, A., Stuart, T., Fleming, L.M., Yeung, B., Rogers, A.J., McElrath, J.M., Blish, C.A., Gottardo, R., Smibert, P., Satija, R., 2021. Integrated analysis of multimodal single-cell data. Cell 184, 3573–3587.e29. https://doi.org/10.1016/j.cell.2021.04.048.
Hardin, P.E., Angerer, L.M., Hardin, S.H., Angerer, R.C., Klein, W.H., 1988. Spec2 genes of Strongylocentrotus purpuratus. J. Mol. Biol. 202, 417–431. https://doi.org/10.1016/0022-2836(88)90275-6.
Hardin, J., Coffman, J.A., McClay, D.R., Black, S.D., 1992. Commitment along the dorsoventral axis of the sea urchin embryo is altered in response to NiCl2. Development 116, 671–685.
Harkey, M.A., Whiteley, H.R., Whiteley, A.H., 1992. Differential expression of the msp130 gene among skeletal lineage cells in the sea urchin embryo: a three dimensional in situ hybridization analysis. Mech. Dev. 37, 173–184. https://doi.org/10.1016/0925-4773(92)90079-Y.
Karlsson, T.M., Arneborg, L., Broström, G., Almroth, B.C., Gipperth, L., Hassellöv, M., 2018. The unaccountability case of plastic pellet pollution. Mar. Pollut. Bull. 129, 52–60. https://doi.org/10.1016/j.marpolbul.2018.01.041.
Kim, B.-M., Rhee, J.-S., Jeong, C.-B., Seo, J.S., Park, G.S., Lee, Y.-M., Lee, J.-S., 2014. Heavy metals induce oxidative stress and trigger oxidative stress-mediated heat shock protein (hsp) modulation in the intertidal copepod Tigriopus japonicus. Comp. Biochem. Physiol. Toxicol. Pharmacol.. 166, 65–74. https://doi.org/10.1016/j.cbpc.2014.07.005.
Kobayashi, N., Okamura, H., 2004. Effects of heavy metals on sea urchin embryo development. 1. Tracing the cause by the effects. Chemosphere 55, 1403–1412. https://doi.org/10.1016/j.chemosphere.2003.11.052.
Koyama, T., Texada, M.J., Halberg, K.A., Rewitz, K., 2020. Metabolism and growth adaptation to environmental conditions in Drosophila. Cell. Mol. Life Sci. 77, 4523–4551. https://doi.org/10.1007/s00018-020-03547-2.
Krzywinski, M., Schein, J., Birol, İ., Connors, J., Gascoyne, R., Horsman, D., Jones, S.J., Marra, M.A., 2009. Circos: an information aesthetic for comparative genomics. Genome Res. 19, 1639–1645. https://doi.org/10.1101/gr.092759.109.
Kudtarkar, P., Cameron, R.A., 2017. Echinobase: an expanding resource for echinoderm genomic information. Database 2017. https://doi.org/10.1093/database/bax074.
Li, H.-X., Getzinger, G.J., Ferguson, P.L., Orihuela, B., Zhu, M., Rittschof, D., 2016. Effects of toxic leachate from commercial plastics on larval survival and settlement of the barnacle Amphibalanus amphitrite. Environ.Sci.Technol. 50, 924–931. https://doi.org/10.1021/acs.est.5b02781.
Li, E., Materna, S.C., Davidson, E.H., 2012. Direct and indirect control of oral ectoderm regulatory gene expression by Nodal signaling in the sea urchin embryo. Dev. Biol. 369, 377–385. https://doi.org/10.1016/j.ydbio.2012.06.022.
Liao, Y., Smyth, G.K., Shi, W., 2014. featureCounts: an efficient general purpose program for assigning sequence reads to genomic features. Bioinformatics 30, 923–930. https://doi.org/10.1093/bioinformatics/btt656.
Love, M.I., Huber, W., Anders, S., 2014. Moderated estimation of fold change and dispersion for RNA-seq data with DESeq2. Genome Biol. 15, 1–21. https://doi.org/10.1186/s13059-014-0550-8.
Martik, M.L., Lyons, D.C., McClay, D.R., 2016. Developmental gene regulatory networks in sea urchins and what we can learn from them [version 1; peer review: 3 approved]. F1000Research, 5 https://doi.org/10.12688/f1000research.7381.1.
Massri, A.J., Greenstreet, L., Afanassiev, A., Berrio, A., Wray, G.A., Schiebinger, G., McClay, D.R., 2021. Developmental single-cell transcriptomics in the Lytechinus variegatus sea urchin embryo. Development 148, dev198614. https://doi.org/10.1242/dev.198614.
Mato, Y., Isobe, T., Takada, H., Kanehiro, H., Ohtake, C., Kaminuma, T., 2001. Plastic resin pellets as a transport medium for toxic chemicals in the marine environment. Environ. Sci. Technol. 35, 318–324. https://doi.org/10.1021/es0010498.
Matranga, V., Zito, F., Costa, C., Bonaventura, R., Giarrusso, S., Celi, F., 2010. Embryonic development and skeletogenic gene expression affected by X-rays in the Mediterranean Sea urchin Paracentrotus lividus. Ecotoxicology 19, 530–537. https://doi.org/10.1007/s10646-009-0444-9.
McClay, D.R., Miranda, E., Feinberg, S.L., 2018. Neurogenesis in the sea urchin embryo is initiated uniquely in three domains. Development 145, dev167742. https://doi.org/10.1242/dev.167742.
Mcintyre, D.C., Lyons, D.C., Martik, M., Mcclay, D.R., 2014. Branching out: origins of the sea urchin larval skeleton in development and evolution. Genesis 52, 173–185. https://doi.org/10.1002/dvg.22756.
Mitsunaga, K., Yasumasu, I., 1984. Stage specific effects of Zn2+ on sea urchin embryogenesis. (animalization/EDDA/EDTA-OH/sea urchin embryos/Zn2+). Dev.Growth Differ. 26, 317–327. https://doi.org/10.1111/j.1440-169X.1984.00317.x.
van der Molen, J., van Leeuwen, S.M., Govers, L.L., van der Heide, T., Olff, H., 2021. Potential micro-plastics dispersal and accumulation in the North Sea, with application to the MSC zoe incident. Front. Mar. Sci. 8. https://doi.org/10.3389/fmars.2021.607203.
Molina, M.D., de Crozé, N., Haillot, E., Lepage, T., 2013. Nodal: master and commander of the dorsal–ventral and left–right axes in the sea urchin embryo. Curr.Opin.Genet.Dev. 23, 445–453. https://doi.org/10.1016/j.gde.2013.04.010.
Nam, J., Su, Y.-H., Lee, P.Y., Robertson, A.J., Coffman, J.A., Davidson, E.H., 2007. Cis-regulatory control of the nodal gene, initiator of the sea urchin oral ectoderm gene network. Dev. Biol. 306, 860–869. https://doi.org/10.1016/j.ydbio.2007.03.033.
Nemer, M., Travaglini, E.C., Rondinelli, E., D'Alonzo, J., 1984. Developmental regulation, induction, and embryonic tissue specificity of sea urchin metallothionein gene expression. Dev. Biol. 102, 471–482. https://doi.org/10.1016/0012-1606(84)90212-4.
Nemer, M., Wilkinson, D.G., Travaglini, E.C., Sternberg, E.J., Butt, T.R., 1985. Sea urchin metallothionein sequence: key to an evolutionary diversity. Proc. Natl. Acad. Sci. 82, 4992–4994. https://doi.org/10.1073/pnas.82.15.4992.
Ogata, Y., Takada, H., Mizukawa, K., Hirai, H., Iwasa, S., Endo, S., Mato, Y., Saha, M., Okuda, K., Nakashima, A., Murakami, M., Zurcher, N., Booyatumanondo, R., Zakaria, M.P., Dung, L.Q., Gordon, M., Miguez, C., Suzuki, S., Moore, C., Karapanagioti, H.K., Weerts, S., McClurg, T., Burres, E., Smith, W., Van, Velkenburg M., Lang, J.S., Lang, R.C., Laursen, D., Danner, B., Stewardson, N., Thompson, R.C., 2009. International Pellet Watch: global monitoring of persistent organic pollutants (POPs) in coastal waters. 1. Initial phase data on PCBs, DDTs, and HCHs. Mar. Pollut. Bull. 58, 1437–1446. https://doi.org/10.1016/j.marpolbul.2009.06.014.
Oliviero, M., Tato, T., Schiavo, S., Fernández, V., Manzo, S., Beiras, R., 2019. Leachates of micronized plastic toys provoke embryotoxic effects upon sea urchin Paracentrotus lividus. Environ. Pollut. 247, 706–715. https://doi.org/10.1016/j.envpol.2019.01.098.
Paganos, P., Caccavale, F., La Vecchia, C., D'Aniello, E., D'Aniello, S., Arnone, M.I., 2022. FISH for all: a fast and efficient fluorescent in situ hybridization (FISH) protocol for marine embryos and larvae. Front. Physiol. 13, 1–9. https://doi.org/10.3389/fphys.2022.878062.
Paganos, P., Voronov, D., Musser, J.M., Arendt, D., Arnone, M.I., 2021. Single-cell RNA sequencing of the Strongylocentrotus purpuratus larva reveals the blueprint of major cell types and nervous system of a non-chordate deuterostome. eLife 10, 1–29. https://doi.org/10.7554/eLife.70416.
Partow, H., Lacroix, C., Le Floch, S., Alcaro, L., 2021. X-Press Pearl Maritime Disaster Sri Lanka Report of the Un Environmental Advisory Mission.
Perillo, M., Oulhen, N., Foster, S., Spurrell, M., Calestani, C., Wessel, G., 2020. Regulation of dynamic pigment cell states at single-cell resolution. eLife 9, e60388. https://doi.org/10.7554/eLife.60388.
Perillo, M., Paganos, P., Spurrell, M., Arnone, M.I., Wessel, G.M., 2021. Methodology for Whole Mount and Fluorescent RNA In Situ Hybridization in Echinoderms: Single, Double, and Beyond. Methods in Molecular Biology (Clifton, N.J.), 195–216 https://doi.org/10.1007/978-1-0716-0974-3_12.
Perillo, M., Wang, Y.J., Leach, S.D., Arnone, M.I., 2016. A pancreatic exocrine-like cell regulatory circuit operating in the upper stomach of the sea urchin Strongylocentrotus purpuratus larva. BMC Evol. Biol. 16, 117. https://doi.org/10.1186/s12862-016-0686-0.
Sundt, Peter, Per-Erik Schultze, F.S., 2014. Sources of Microplastic - Pollution to the Marine Environment. Mepex, Norwegian Environment Agency, pp. 1–108.
Provencher, J.F., Bond, A.L., Mallory, M.L., 2015. Marine birds and plastic debris in Canada: a national synthesis and a way forward. Environ. Rev. 23, 1–13. https://doi.org/10.1139/er-2014-0039.
Qu, R., Feng, M., Wang, X., Qin, L., Wang, C., Wang, Z., Wang, L., 2014. Metal accumulation and oxidative stress biomarkers in liver of freshwater fish Carassius auratus following in vivo exposure to waterborne zinc under different pH values. Aquat. Toxicol. 150, 9–16. https://doi.org/10.1016/j.aquatox.2014.02.008.
Ragusa, M.A., Nicosia, A., Costa, S., Cuttitta, A., Gianguzza, F., 2017. Metallothionein gene family in the sea urchin Paracentrotus lividus: gene structure, differential expression and phylogenetic analysis. Int. J. Mol. Sci. 18. https://doi.org/10.3390/ijms18040812.
Ransick, A., Davidson, E.H., 2006. Cis-regulatory processing of Notch signaling input to the sea urchin glial cells missing gene during mesoderm specification. Dev. Biol. 297, 587–602. https://doi.org/10.1016/j.ydbio.2006.05.037.
Rendell-Bhatti, F., Paganos, P., Pouch, A., Mitchell, C., D'Aniello, S., Godley, B.J., Pazdro, K., Arnone, M.I., Jimenez-Guri, E., 2020. Developmental toxicity of plastic leachates on the sea urchin Paracentrotus lividus. Environ. Pollut. 269, 115744. https://doi.org/10.1016/j.envpol.2020.115744.
Rizzo, F., Fernandez-Serra, M., Squarzoni, P., Archimandritis, A., Arnone, M.I., 2006. Identification and developmental expression of the ets gene family in the sea urchin (Strongylocentrotus purpuratus). Dev. Biol. 300, 35–48. https://doi.org/10.1016/j.ydbio.2006.08.012.
Rochman, C.M., Brookson, C., Bikker, J., Djuric, N., Earn, A., Bucci, K., Athey, S., Huntington, A., Mcllwraith, H., Munno, K., De Frond, H., Kolomijeca, A., Erdle, L., Grbic, J., Bayoumi, M., Borrelle, S.B., Wu, T., Santoro, S., Werbowski, L.M., Zhu, X., Giles, R.K., Hamilton, B.M., Thaysen, C., Kaura, A., Klasios, N., Ead, L., Kim, J., Sherlock, C., Ho, A., Hung, C., 2019. Rethinking microplastics as a diverse contaminant suite. Environ. Toxicol. Chem. 38, 703–711. https://doi.org/10.1002/etc.4371.
Ruttkay-Nedecky, B., Nejdl, L., Gumulec, J., Zitka, O., Masarik, M., Eckschlager, T., Stiborova, M., Adam, V., Kizek, R., 2013. The role of metallothionein in oxidative stress. Int. J. Mol. Sci. 14, 6044–6066. https://doi.org/10.3390/ijms14036044.
Saudemont, A., Haillot, E., Mekpoh, F., Bessodes, N., Quirin, M., Lapraz, F., Duboc, V., Röttinger, E., Range, R., Oisel, A., Besnardeau, L., Wincker, P., Lepage, T., 2010. Ancestral regulatory circuits governing ectoderm patterning downstream of nodal and BMP2/4 revealed by gene regulatory network analysis in an echinoderm. PLoS Genet. 6, e1001259. https://doi.org/10.1371/journal.pgen.1001259.
Sewwandi, M., Hettithanthri, O., Egodage, S.M., Amarathunga, A.A.D., Vithanage, M., 2022. Unprecedented marine microplastic contamination from the X-press pearl container vessel disaster. Sci. Total Environ. 828, 154374. https://doi.org/10.1016/j.scitotenv.2022.154374.

Sherrington, C., 2016. Plastics in the marine environment. Report to European Commission. Eunomia, pp. 1–13.

Slota, L.A., McClay, D.R., 2018. Identification of neural transcription factors required for the differentiation of three neuronal subtypes in the sea urchin embryo. Dev. Biol. 435, 138–149. https://doi.org/10.1016/j.ydbio.2017.12.015.

Sun, Q., Li, Y., Shi, L., Hussain, R., Mehmood, K., Tang, Z., Zhang, H., 2022. Heavy metals induced mitochondrial dysfunction in animals: molecular mechanism of toxicity. Toxicology 469, 153136. https://doi.org/10.1016/j.tox.2022.153136.

Supek, F., Bošnjak, M., Škunca, N., Šmuc, T., 2011. REVIGO summarizes and visualizes long lists of gene ontology terms. PLoS ONE 6, e21800. https://doi.org/10.1371/journal.pone.0021800.

Teuten, E.L., Saquing, J.M., Knappe, D.R.U., Barlaz, M.A., Jonsson, S., Bjorn, A., Rowland, S.J., Thompson, R.C., Galloway, T.S., Yamashita, R., Ochi, D., Watanuki, Y., Moore, C., Viet, P.H., Tana, T.S., Prudente, M., Boonyatumanond, R., Zakaria, M.P., Akkhavong, K., Ogata, Y., Hirai, H., Iwasa, S., Mizukawa, K., Hagino, Y., Imamura, A., Saha, M., Takada, H., 2009. Transport and release of chemicals from plastics to the environment and to wildlife. Philos. Trans. R. Soc., B Biol. Sci. 364, 2027–2045. https://doi.org/10.1098/rstb.2008.0284.

Thompson, J.R., Paganos, P., Benvenuto, G., Arnone, M.I., Oliveri, P., 2021. Post-metamorphic skeletal growth in the sea urchin Paracentrotus lividus and implications for body plan evolution. EvoDevo 12, 3. https://doi.org/10.1186/s13227-021-00174-1.

Thushari, G.G.N., Senevirathna, J.D.M., 2020. Plastic pollution in the marine environment. Heliyon 6, e04709. https://doi.org/10.1016/j.heliyon.2020.e04709.

Tu, Q., Cameron, R.A., Davidson, E.H., 2014. Quantitative developmental transcriptomes of the sea urchin Strongylocentrotus purpuratus. Dev. Biol. 385, 160–167. https://doi.org/10.1016/j.ydbio.2013.11.019.

Turner, A., Wallerstein, C., Arnold, R., 2019. Identification, origin and characteristics of biobead microplastics from beaches in western Europe. Sci. Total Environ. 664, 938–947. https://doi.org/10.1016/j.scitotenv.2019.01.281.

Walther, U.I., Walther, S.C., Mückter, H., Fichtl, B., 2008. Enhancing glutathione synthesis can decrease zinc-mediated toxicity. Biol. Trace Elem. Res. 122, 216–228. https://doi.org/10.1007/s12011-007-8072-9.

Wang, H., Ding, J., Ding, S., Chang, Y., 2019. Metabolomic changes and polyunsaturated fatty acid biosynthesis during gonadal growth and development in the sea urchin Strongylocentrotus intermedius. Comp. Biochem. Physiol. Part D Genomics Proteomics 32, 100611. https://doi.org/10.1016/j.cbd.2019.100611.

Wang, C., Hou, M., Shang, K., Wang, H., Wang, J., 2022. Microplastics (polystyrene) exposure induces metabolic changes in the liver of rare minnow (Gobiocypris rarus). Molecules 27. https://doi.org/10.3390/molecules27030584.

Wright, S.L., Rowe, D., Thompson, R.C., Galloway, T.S., 2013. Microplastic ingestion decreases energy reserves in marine worms. Curr. Biol. 23, R1031–R1033. https://doi.org/10.1016/j.cub.2013.10.068.